

STOCK REMOVAL RATES IN INTERNAL
GRAINDING: A MODEL OF THE PROCESS

2122 NT
3/21
2001

by

RICHARD P. LINDSAY

S.B., Northeastern University
(1965)

Submitted in Partial Fulfillment
of the Requirements for the
Degree of Master of
Science
at the
Massachusetts Institute of Technology

August 1966

Signature of Author **Signature redacted**
 Department of Mechanical Engineering
 August 22, 1966

Certified by **Signature redacted**
 Thesis Supervisor

Accepted by **Signature redacted**
 Chairman, Departmental Committee
 on Graduate Students

MRL



STOCK REMOVAL RATES IN INTERNAL
GRAINDING: A MODEL OF THE PROCESS

*Thesis
M.E.
1966*

RICHARD S. LINDSAY

S.B., Northeastern University
(1965)

Submitted in Partial Fulfillment
of the Requirements for the
Degree of Master of
Science
at the
Massachusetts Institute of Technology

August 1966

..... Signature of Author *Richard S. Lindsay*

..... Department of Mechanical Engineering
..... August 22, 1966

..... Certified by *[Signature]*
..... Thesis Supervisor

..... Accepted by *[Signature]*
..... Chairman, Departmental Committee
..... on Graduate Students

STOCK REMOVAL RATES IN INTERNAL GRINDING:
A MODEL OF THE PROCESS

by

Richard P. Lindsay

Submitted to the Department of
Mechanical Engineering on August 22, 1966
in partial fulfillment of the
requirements for the degree of
Master of Science

A model of the grinding process is given in which the cutting and sliding regions of a worn grain are separated from each other. It is assumed that each of these processes can be represented by use of constant stresses in the normal and tangential directions resulting in four unknown constants. Using four experimental data points and the relation between the tangential and normal force, the four constants are determined. The theory then is seen to fit a total of fifty-nine experimental results.

The constants thus determined are seen to be compatible with results obtained with single-grain sliding tests.

Thesis Supervisor: Nathan H. Cook
Professor of Mechanical Engineering

CONTENTS

Introduction

Definition Of Terms Used

A. Models Of The Process

1-Constant Stress

2-Elastic Rebound

B. Analytical Quantities

1-Random Array Of Grains

2-Spacing Of Effective Grains (s)

3-Grain Density (C)

4-Length Of Contact (L_c)

5-Diameter Of Worn Flat (\bar{a})

6-Shape Of Cut in Internal Grinding

a.-Condition for Scallop-shaped Cut

b.-Determination of the Depth of Cut ($\frac{t}{d}$)

c.-Determination of the Width of Cut (b)

7-Force Per Grain (F_{ng})

C. Mathematical Development of Constant-Stress Model

1-General Solution in Normal Direction

2-General Solution in Tangential Direction

3-General Solution for the Rate of Hole-Radius Growth (\bar{v})

D. Experimental Quantities

1-Normal and Tangential Forces (F_n, F_s)

2-Total Instantaneous Contact Area (A_{rl})

3-Instantaneous Rate of Hole-Radius Growth (\bar{v})

4-Proof of Scallop-shape Cut Assumption

CONTENTS (CONTINUED)

E. Solution of Constant-Stress Model

1-Tests Using 60 Grit Grinding Wheel

a.-Normal Direction : k_1^{60} and k_2^{60} b.-Tangential Direction : k_3^{60} and k_4^{60}

2-Tests Using 90 Grit Grinding Wheel

a.-Normal Direction : k_1^{90} and k_2^{90} b.-Tangential Direction : k_3^{90} and k_4^{90} 3-Solution of \bar{v} Using Constants4- $\frac{\bar{v}}{F_n}$ vs. σ as a Linear Function

F. Comparison of the Constants with Single-Grain Sliding Tests

G. Conclusions

Appendices

INTRODUCTION

It has been found that the cutting ability of a grinding wheel diminishes with time from a high initial value to a lower relatively-constant rate, when the constant applied force between the wheel and the work is low enough to prevent gross breakdown of the wheel. Microscopic examination of the wheel surface, at various stages in the process, reveal that the flats worn on the wheel grains continually grow with time. Thus, if the area of these flats in contact with the work is measured and the normal force of grinding is known, the relation between cutting ability of the wheel and actual applied normal stress may be determined empirically.

When this was done it was found that the removal ability, \bar{v} , when divided by applied force, F_n , varied linearly with the applied normal stress, σ .

The purpose of this thesis then is to derive theoretically the above relationship or to show how such a linear approximation can represent the true relationship.

Definition of Terms Used

- d = Average diameter of grain in the wheel (INCH)
- F_n = Normal force between wheel and work (LB)
- F_s = Tangential force between wheel and work (LB)
- F_{Ng} = Normal force on a grain (LB)
- F_{sg} = Tangential force on a grain (LB)
- A_{RP} = Total real contact area in photo strip of length, . (IN²)
- A_{RL} = Total real area in contact between the wheel and work (IN²)
- \bar{r} = Instantaneous rate of hole radius growth
(internal grinding) $\frac{\text{INCH}}{\text{SEC}}$
- G = Grain density of the wheel $\frac{\text{GRAINS}}{\text{INCH}^2}$
- \bar{s} = Distance from one effective grain to the next,
measured in a circumferential arc, in any
random plane through the wheel $\frac{\text{INCH}}{\text{GRATN}}$
- l = Width of photographic strip of wheel surface (INCH)
- \bar{a} = Instantaneous diameter of the flat on any grain
(assuming round flats) (INCH)
- σ = F_n/A_{RL} actual applied normal stress (psi)
- W = Width of workpiece (INCH)
- L_c = Length of contact of wheel and work under a given
normal force, F_n (INCH)

D = Diameter of wheel (INCH)

D_w = Diameter of work (INCH)

V = Peripheral surface speed of wheel $\frac{\text{INCH}}{\text{SEC}}$

n = Rotational speed of work $\frac{\text{REV}}{\text{SEC}}$

N = Rotational speed of wheel $\frac{\text{REV}}{\text{SEC}}$

t = Average grain depth of cut (INCH)

k_1, k_2 = Constants

A. Models of the Process

I. Constant-Stress

Consider Figure 1: it is assumed that the stock-removal process can be divided into two zones: the cutting region where the chip is produced and the sliding region under the worn grain flat. Then the following assumptions will be made:

a.- Chip formation is continuous and a zone of rigid-plasticity exists. Then the forces of cutting may be written.

$$F_V = k_1^* bt \cot \phi \quad (1)$$

$$F_H = k_3^* bt$$

that is the forces in the cutting region are proportional to the depth and width of cut, t .

b.- The sliding forces are assumed as:

$$F_V = k_2^* \frac{\pi a^2}{4} \quad (2)$$

$$F_H = k_4^* \frac{\pi a^2}{4}$$

That is, constant stresses exist under the grain flat and are independent of the depth of cut.

Thus the normal force may be written as:

$$F_N = F_{\text{cutting}} + F_{\text{sliding}} \quad (3)$$

$$F_{Ng} = k_1^* bt \cot \phi + k_2^* \frac{\pi a^2}{4}$$

$$\text{Letting } k_1 = k_1^* \cot \emptyset$$

$$\text{and } k_2 = \frac{\pi}{4} k_2^*$$

(3) becomes:

$$F_{Ng} = k_1 bt + k_2 \bar{a}^{-2} \quad (4a)$$

$$\text{or } i = \frac{1}{F_{Ng}} \left[k_1 bt + k_2 \bar{a}^{-2} \right] \quad (4b)$$

The forces in the tangential direction may be written as:

$$F_{sg} = k_3^* bt + k_4^* \frac{\pi \bar{a}^{-2}}{4} \quad (5)$$

$$\text{Letting } k_3 = k_3$$

$$\text{and } k_4 = k_4^* \left(\frac{\pi}{4} \right)$$

$$\text{and defining } F_{sg} = \mu F_{Ng}$$

(5) becomes:

$$\mu F_{Ng} = k_3 bt + k_4 \bar{a}^{-2} \quad (6a)$$

$$\text{or } \mu = \frac{1}{F_{Ng}} \left[k_3 bt + k_4 \bar{a}^{-2} \right] \quad (6b)$$

Note similarity between (4b) and (6b) where only μ and constants vary.

2. Elastic Rebound:

Again considering Figure 1, assume the following:

a.- At the cutting region:

$$F_V = k_1^* bt \cot \emptyset$$

$$F_H = k_3^* bt$$

Same as the first model

b.- Under the grain flat:

$$F_V = k_2^* \bar{a} bt$$

$$F_H = k_4^* \bar{a} bt$$

it being now assumed that the forces imposed on the grain flat are proportional to the length, width and depth of cut. That is, these forces are proportional to the elastic rebound of the distorted metal in the shear zone. Then, as before, writing the normal force as:

$$F_{Ng} = k_1^* bt \cot \emptyset + k_2^* \bar{a} bt$$

Letting $k_1 = k_1^* \cot \emptyset$

and $k_2 = k_2^*$

Then $F_{Ng} = bt (k_1 + k_2 \bar{a})$

or $l = \frac{bt}{F_{Ng}} (k_1 + k_2 \bar{a})$

This model was found to produce a tensile constant, k_1 meaning that the normal stress under the grain is too large under this assumption. Appendix 8 will follow the development of this assumption.

The next sections will be concerned with the determining the quantities necessary for the deriving of working formulas from the relations 4b and 6b.

B. Analytical Quantities

1. Random Array of Grains

In order to establish the quantities C , grain density of the wheel and \bar{S} , effective grain spacing around the wheel periphery in a plane, the grain array of Figure 2 is used.

The wheel surface is assumed to have the array shown where: "M" is the distance between grains on any ring, k: "L" is the distance between rings; \bar{a} is the diameter of the flat worn onto the grain at any time.

2. Spacing of Effective Grains, \bar{S} :

Consider a line drawn from the origin, "0", in a radial direction. The average distance travelled along such a line is when the probability of intersecting another grain flat equals the probability of missing another flat (i.e. the escaping probability equals 0.5). It may be shown (Appendix 1) that the average distance so travelled is given by (Appendix formula 1.2.6):

$$\bar{S} = \frac{L^2}{\bar{a}} \quad (7)$$

which states that as \bar{a} becomes larger (as the real area grows) the effective grain spacing becomes smaller since L is a constant, which will now be determined.

Figures 4 and 5, while they present a picture of the cutting surface of the wheel, also give the distance between effective grains, because if the grain has become worn it was in contact with

the work and so was an "effective grain". Thus an average of the distance between flats from Figure 5 will be a measure of L , when any one flat is considered as the origin. From Figure 5 measurements, for the 60 grit wheel, the average spacing is 0.018 inch. Since the average size of a 60 grit size stone is 0.016 inch, assume the spacing may be given as:

$$L \approx d \quad (8)$$

Then (7) becomes

$$\bar{S} = \frac{d^2}{\bar{a}} \quad (9)$$

Now the grain density, C , may be determined.

3. Grain Density, C

Referring to Figure 2, in the first ring, the number of grains per area is:

$$C = \frac{\text{number of grains}}{\text{area}}$$

$$C = \frac{1 + (1/2)(6)}{\pi L^2}$$

$$C = \frac{1.26}{L^2} \quad (10)$$

or using (8):

$$C = \frac{1.26}{d^2} \quad (11)$$

Thus the grain density increases with smaller grain sizes.

4. Length of Contact, L_c :

The assumption that the workpiece is infinitely stiff, relative to the wheel is made to begin. It is also found that due to the assumed array, the number of grains in contact with the work increases linearly with the length of contact. Thus, as the normal force is increased more and more grains come into contact with the work and if it assumed that the bonding-agent holding the grains in the wheel acts as a spring, then the applied force, F_N , is being resisted by more and more spring-loaded grains. Hence the deflection of the wheel in the direction parallel to F_N is not linear with the applied force, F_N , which it would be if only the original number of grains were present for all deflections.

From the assumption that the slope of the force-deflection curve is always a multiple of the original slope (the slope increasing as more and more grains come into contact at higher forces) the following relationship is derived (see Appendix 2):

$$L_c = \left[\frac{d D D_w F_N}{m k_g (D_w - D)} \right]^{1/3} \quad (12)$$

Where:

$$M_{60 \text{ grit wheel}} = 0.2 \text{ dimensionless}$$

$$M_{90} = 0.167$$

$$k_{60} = 1.025 (10^5) \frac{\text{LB}}{\text{INCH}}$$

$$k_{90} = 0.266 (10^5) \frac{\text{LB}}{\text{INCH}}$$

5. Diameter of Worn Grain Flat (\bar{a}):

The total instantaneous real area in contact, A_{RL} , is merely the sum of the flats worn onto the number of grains in contact.

Thus, A_{RL} may be written as:

$$A_{RL} = (\text{No. grains in contact}) \left(\frac{\text{area}}{\text{grain}} \right)$$

$$A_{RL} = C \cdot L_c \cdot W \left(\frac{\pi \bar{a}^2}{4} \right) \quad \frac{\text{grains}}{\text{inch}^2} \cdot \text{inch} \cdot \text{inch} \cdot \frac{\text{inch}^2}{\text{grain}}$$

Considering the worn flat to be circular.

Using (11) and (12), the above becomes:

$$A_{RL} = \left(\frac{1.26}{d^2} \right) W \left(\frac{\pi \bar{a}^2}{4} \right) \left[\frac{d D D_w F_N}{m k_g (D_w - D)} \right]^{1/3}$$

$$\left(\frac{\bar{a}}{d} \right)^2 = \frac{4 A_{RL}}{1.26 \pi W} \left[\frac{m k_g (D_w - D)}{d D D_w F_N} \right]^{1/3}$$

$$\left(\frac{\bar{a}}{d} \right) = \left(\frac{A_{RL}}{W} \right)^{1/2} \cdot \left[\frac{m k_g (D_w - D)}{d D D_w F_N} \right]^{1/6} \quad (13a)$$

or

$$\bar{a} = \left(\frac{A_{RL}}{W} \right)^{1/2} \cdot d^{5/6} \cdot \left[\frac{m k_g (D_w - D)}{D D_w F_N} \right]^{1/6} \quad (13b)$$

6. Shape of Cut in Internal Grinding

a. Condition for Scalloped-Shaped Cut:

Consider Figure 6 wherein is shown a plane section of the wheel, with grits spaced on the plane periphery, \bar{S} distance apart. The normal force will cause a penetration into the work as shown but a grain may or may not be present at the interference region, L_c .

The shape of the chip produced, as motions v and V are introduced, will be scalloped as shown if the following condition exists:

$$\frac{N}{v} < \frac{\bar{S}}{V} \quad (14)$$

or

$$\frac{v}{V} > \frac{N}{\bar{S}}$$

Experimental data will prove this condition to be valid. Also generally, from the geometry of Figure 6:

$$N = 2\sqrt{tD} \quad (15)$$

also

$$A_{cut} = \frac{3}{2} t^{3/2} D^{1/2} \quad (16)$$

b. Determination of Depth of Cut t :

Considering continuity of the stock-removal process from Figure 6, the area removal per unit time may be written two ways:

1. from the fact that \bar{r} is the rate of radius growth,
then the area removed per unit time is:

$$\bar{r} (\pi D_w)$$

2. Also the amount of material removed must be equal
to the number of cuts per unit time multiplied by
the area removed per cut, or:

$$\left(\frac{V}{S}\right) \cdot A \text{ cut}$$

Thus, for continuity these two rates must be equal:

$$\pi D_w \bar{r} = \left(\frac{V}{S}\right) \cdot A \text{ cut}$$

Using (9) and (16):

$$\pi D_w \bar{r} = \frac{V \bar{a}}{d^2} \left(\frac{3}{2} t^{3/2} D^{1/2}\right)$$

$$t = \left[\frac{2\pi D_w \bar{r} d^2}{3 D^{1/2} V \bar{a}} \right]^{2/3} \quad (17)$$

Using (13a) and dividing both sides by "d":

$$\left(\frac{t}{d}\right) = \left\{ \frac{2\pi D_w \bar{r} d}{3 D^{1/2} V d^{3/2}} \left(\frac{W}{A_{RL}}\right)^{1/2} \cdot \left[\frac{d D D_w F_N}{m k_g (D_w - D)} \right]^{1/6} \right\}^{2/3}$$

yielding:

$$\left(\frac{t}{d}\right) = 1.635 \left(\frac{\bar{r}}{V}\right)^{2/3} \cdot \left(\frac{W}{A_{RL}}\right)^{1/3} \cdot \left[\frac{F_N D_w^7}{m k_g (D_w - D)(Dd)^2} \right]^{1/9} \quad (18)$$

C. Determination of the Width of Cut (b):

Consider Figure 7 where b is the width of cut of a ploughed groove made by a grain with flat, \bar{a} . From continuity the volume removed per unit time may be written two ways:

1. Considering \bar{v} , the rate of hole radius growth, the volume removed is:

$$\bar{v} (\pi D_w) (W)$$

2. Also the total volume removed must be equal to the volume removed per cut times the number of cuts per unit time:

$$WV \left(\frac{A_{\text{cut}}}{b} \right) \left(\frac{\text{CUTTERS}}{\text{SECOND}} \right) \cdot \left(\frac{\text{VOLUME}}{\text{CUT}} \right)$$

These must be equal. Using (11) and (16):

$$b = \frac{\bar{v} \pi D_w W}{WV \left(\frac{1.26}{d^2} \right) \left[\frac{3}{2} t^{3/2} D^{1/2} \right]}$$

Using (17):

$$b = \frac{\pi \left(\frac{2}{3} \right) \bar{v} D_w d^2}{1.26 \left(\frac{3}{d^2} \right) V D^{1/2} \left\{ \left[\frac{2 \pi D_w \bar{v} d^2}{3 D^{1/2} V a} \right]^{2/3} \right\}^{3/2}}$$

$$b = \bar{a} / 1.26$$

$$b = 0.8 \bar{a}$$

(19)

7. Force per Grain, F_{Ng}

Define

$$F_{Ng} \equiv \frac{F_N}{\text{No. of grains in contact}}$$

$$F_{Ng} = \frac{F_N}{(C)(L_c)(W)}$$

Using (11) and (12):

$$\left(\frac{F_{Ng}}{F_N}\right) = \frac{d^2}{1.26W} \left[\frac{mkg(D_w - D)}{dDD_w F_N} \right]^{1/3}$$

or

$$\left(\frac{F_{Ng}}{F_N}\right) = \frac{0.294}{W} \left[\frac{mkg(D_w - D)d^6}{DD_w F_N d} \right]^{1/3} \quad (20)$$

C. Mathematical Development of Constant Stress Model

1. General Solution in Normal Direction:

Since all the necessary parameters are now described mathematically, the development of the theory may be carried out. Copying formula 4b below:

$$1 = \frac{1}{F_{Ng}} \left[k_1 b t + k_2 \bar{a}^2 \right] \quad (4b)$$

Using (19), (20), (13a) and (18) (see Appendix 3) it is found that

$$1 = \frac{4.45 k_1 W^{5/6}}{F_N^{5/9} \sigma^{1/6}} \left[\frac{D_w^{17}}{m^5 k_g^5 (D_w - D)^5 (Dd)} \right]^{1/18} \left(\frac{\bar{\sigma}}{V} \right)^{2/3} + 3.4 \frac{k_2}{\sigma} \quad (21)$$

2. General Solution in Tangential Direction:

Comparing the form of 4b and 6b, noting the only changes are and the constants, the solution in the tangential direction may be written from (21) as:

$$\mu = \frac{4.45 k_3 W^{5/6}}{F_N^{5/9} \sigma^{1/6}} \left[\frac{D_w^{17}}{m^5 k_g^5 (D_w - D)^5 (dD)} \right]^{1/18} \left(\frac{\bar{\sigma}}{V} \right)^{2/3} + 3.4 \frac{k_4}{\sigma} \quad (22)$$

3. General Solution for Rate of Radius Growth, \bar{r} :

Returning now to (21) and solving for $\left(\frac{\bar{r}}{V}\right)^{2/3}$ yields:

$$\left(\frac{\bar{r}}{V}\right)^{2/3} = \left\{ 1 - 3.4 \frac{k_2}{\sigma} \right\} \left\{ \frac{\sigma^{1/6} F_N^{5/9} \left[\frac{dD (m k_g [D_w - D])^5}{D_w^{17}} \right]^{1/18}}{4.45 k_1 W^{5/6}} \right\} \quad (23)$$

Revising this as per Appendix 4, yields:

$$\left(\frac{\bar{r}}{V}\right) = \frac{0.106 [dD (m k_g [D_w - D])^5]^{1/12}}{k_1^{3/2} W^{5/4} D_w^{17/12} F_N^{5/12} A_{RL}^{1/4}} \left(F_N - 3.4 k_2 A_{RL} \right)^{3/2} \quad (24)$$

where the last parenthesis is the potential force available for cutting, F_N , minus the force being absorbed under the flat. Thus, as the grain flats grow the potential cutting force is diminished by the force under the flat, causing the cutting rate \bar{r} to diminish.

From (24) it may be noted that

$$\left(\frac{\bar{r}}{V}\right) = 0 \quad \text{when} \quad \left\{ F_N - 3.4 k_2 A_{RL} \right\} = 0$$

or

$$\sigma_0 = 3.4 k_2 \quad (25)$$

Thus σ_0 , the stress at which the wheel will cease to cut, is 3.4 times the constant normal stress assumed to exist under the grain flat.

Summarizing then: a model has been assumed for which the cutting forces are proportional to the depth and width of cut and the sliding forces are independent of the depth of cut but proportional to the worn flat area on the grains.

Using this model, formulas have been derived which contain various constants. Using four experimental results, these constants will be evaluated and the resultant formulas used to predict other experimental results. Specifically, formula (21) will be solved using two data points for each wheel, 60 and 90 grit. Since $\bar{\tau}$ and σ appear in (21) it is necessary to have grinding data for which $\bar{\tau}$ and σ are known. Using the evaluated constants, formula (24) may be used to predict other results.

It should be remembered that the scallop-shaped cut assumption remains to be proven. This will be done when the experimental procedure and data have been given.

D. Experimental Quantities

1. Normal and Tangential Forces:

The test grinding was done under constant normal force, plunge-cut conditions. Thus the normal force was an adjustable and independent variable. Tangential forces were approximated from torque measurements. Generally, for a sharp wheel,

$$\frac{F_S}{F_N} \approx 0.5; \text{ and for a wheel which has become dull, } \frac{F_S}{F_N} \approx 0.3.$$

Figure 8 illustrates these forces.

2. Total Instantaneous Real Area in Contact:

The used wheel was mounted on the bed of a 175-power microscope and the wheel surface was brought into focus. A Polaroid picture was taken at this location. The bed was moved axially the width of the photograph, and another picture was taken at this new location. In this manner a group of photos were obtained, which, when mounted together consecutively, gave a picture of the wheel surface at 175 magnification. Figure 9 illustrates this method; Figure 4 is a reproduction of one such photo and Figure 5 is a reproduction of three such strips, (at a smaller scale of reproduction).

However, the length of the resulting photographic strip, "*l*" in Figure 5, is not necessarily the length of the zone of wheel-work contact under the normal force. Hence this length, L_c , must be determined. A workpiece was finished to a smooth surface by polishing and a wheel was placed in the hole and the normal forces used in grinding, were placed on the wheel-work system (all on the

test machine). Now the wheel was moved 0.010 Inch axially causing the wheel to scratch the work surface. The average width of the "scratch band" was then taken as the width of contact, L_c . See Figure 10, a, b.

Using two of these data points and the deflection hypothesis of this report the formula for the length of contact has been found and is repeated here:

$$L_c = \left[\frac{d D D_w F_N}{m k_g (D_w - D)} \right]^{1/3} \quad (12, \text{repeated})$$

or

$$L_c = \left[\frac{d F_N}{m k_g \left(\frac{1}{D} - \frac{1}{D_w} \right)} \right]^{1/3}$$

The theoretical and experimental results are given in Figure 18D.

Therefore, from the photographic strips (as Figure 5) of the wheel surface, the area in the strip may be measured using a planimeter. Then the real area in the length of contact, assuming the picture strip is representative of any strip on the wheel, is:

$$A_{RL} = \frac{L_c}{l} A_{RP}$$

When the troichoidal equations of motion of the wheel are considered¹, the length of contact L_c is changed less than 1%, therefore the above manner of measuring A_{RL} was used.

3. Instantaneous Rate of Radius Growth \bar{v} :

The rate of growth of the work diameter was measured as shown in Figure 11. A work-riding finger probe, spring-loaded against the work surface was used and its motion was sensed with a Microtrol Electronic gage (1 Division = 10×10^{-6} (in) maximum sensitivity). The motion of the Microtrol gage was fed into a recorder to obtain a tape of the position of the probe versus time. Then, as Figure 11 illustrates, the slope of the position versus time plot, is \bar{v} . The system was sufficiently sensitive to allow \bar{v} measurements to within $\pm 5 \frac{\text{Microinches}}{\text{Second}}$.

Tables 1, 2 and 3 gives the experimental data obtained. Thus the experimental data was collected, and values of σ , for various \bar{v} rates, were obtained.

The theory hinges on the assumption of the scallop-shaped cut and now that the experimental data has been introduced, this assumption will be proven.

4. Proof of Scallop-Shaped Cut Assumption

The condition for scallop-shaped cuts is copied for convenience:

$$\frac{v}{V} > \frac{N}{S} \quad (14, \text{ repeated})$$

Using already derived relations (14) becomes (see Appendix 5):

(1) HAHN, ROBERT S. "ON THE NATURE OF THE GRINDING PROCESS"
PERGAMON PRESS, LONDON, 1963.

$$\frac{\bar{v}}{V} > 2.56 \left[\frac{(DD_w)^2 mkg (D_w - D)}{F_N d^7} \right]^{1/9} \cdot \left(\frac{A_{RL} \bar{v}}{W V} \right)^{1/3} \quad (25)$$

From the experiments:

Case 1: When the wheel is cutting slowly:

$$\bar{v} = 75 \times 10^{-6} \frac{\text{inch}}{\text{sec}}; A_{RL} = 728 \times 10^{-6} \text{ inch}^2$$

$$d_{60} = 0.016 \text{ inch}; D = 1.87 \text{ inch}; D_w = 2.37 \text{ inch}$$

$$M_{60} = 0.2; k_{60} = 1.025 (10^5) \frac{\text{LB}}{\text{INCH}}; F_N = 15 \text{ LB}$$

$$W = 0.250 \text{ inch}; V = 1430 \frac{\text{inch}}{\text{sec}}; \bar{v} = 224 \frac{\text{inch}}{\text{sec}}$$

Into (25):

$$\frac{224}{1430} > 2.56 \left[\frac{(1.87 [2.37])^2 \cdot 0.2 (1.025 \times 10^5) (2.37 - 1.87)}{15 (0.016)^7} \right]^{1/9} \cdot \left[\frac{(728 \times 10^{-6}) (75 \times 10^{-6})}{\left(\frac{1}{4}\right) (1430)} \right]^{1/3}$$

Yields:

$$0.156 > 0.128$$

Case 2: When wheel is cutting at a rapid rate

$$\bar{v} = 440 \times 10^{-6} \frac{\text{inch}}{\text{sec}}; A_{RL} = 126 \times 10^{-6} \text{ inch}^2$$

All other values the same

$$0.156 > 2.56 \left[\frac{(1.87[2.37])^2 \cdot 0.2 (1.025 \times 10^5) (2.37 - 1.87)}{15 (0.016)^7} \right]^{1/9} \cdot \left[\frac{(440 \times 10^{-6}) (126 \times 10^{-6})}{(\frac{1}{4}) (1430)} \right]^{1/3}$$

$$0.156 > 0.129$$

Thus for both fast and slow stock removal the scallop-shaped assumption holds.

E. Solution of Exercise

E. SOLUTION OF CONSTANT-STRESS MODEL

I. Tests Using 60 Grit Wheel

a. Normal Direction: k_1^{60} and k_2^{60} :

Since (21) contains the two unknowns, k_1 and k_2 , two experimental results must be used to evaluate these constants.

Case 1: Wheel is cutting rapidly and σ is large:

$$\bar{v} = 440 \times 10^{-6} \frac{\text{INCH}}{\text{SECOND}}; \sigma = 118000 \text{ psi};$$

$$F_N = 15 \text{ LB}; W = .250 \text{ IN}; D_N = 2.37 \text{ inch};$$

$$M = 0.2; k_g = 1.025 \left((10^5) \frac{\text{LB}}{\text{IN}} \right); D = 1.87 \text{ inch};$$

$$d = 0.016 \text{ in}; V = 1430 \frac{\text{IN}}{\text{SEC}}; (21) \text{ becomes:}$$

$$1 = \frac{4.45 k_1 \left(\frac{1}{4}\right)^{5/6}}{(15)^{5/9}} \frac{2.37^{17}}{(118,000)^{1/6}} \left[\frac{2.37^{17}}{(0.2)^5 (1.025 \times 10^5)^5 (2.37 - 1.87)^5 (1.87)(.016)} \right]^{1/18} \\ + \frac{\left(\frac{440 \times 10^{-6}}{1430}\right)^{2/3}}{118,000} + 3.4 \frac{k_2}{118,000}$$

yielding

$$k_2 + 14.8(10^{-3}) k_1 = 3.47(10^4) \quad (26)$$

Case 2: Wheel is dulled and cutting slowly, σ is reduced

by the growth of flat area:

$$\bar{v} = 75 \times 10^{-6} \frac{\text{IN}}{\text{SEC}}; \sigma = 20630 \text{ psi other values}$$

as above, (21) becomes:

$$1 = \frac{4.45 k_1}{(15)^{5/9}} \left(\frac{1}{4}\right)^{5/6} \frac{2.37^{17/18}}{(20630)^{1/6}} \left[\frac{1}{(0.2)(1.025 \times 10^5)(2.37-1.87)} \right]^{5/18} \frac{(75 \times 10^{-6})^{2/3}}{[1.87(.016)]^{1/18}} \cdot \left(\frac{1}{1430}\right)^{2/3} + 3.4 \frac{k_2}{20630}$$

yielding

$$k_2 + 1.06 (10^{-3}) k_1 = 0.608 (10^4) \quad (27)$$

solving (26) and (27) simultaneously gives the constants:

$$k_1^{60} = 2.08 (10^{-6}) \text{ psi}$$

$$k_2^{60} = 3900 \text{ psi}$$

b. Tangential Direction: k_3^{60} and k_4^{60} :

Equation (22) contains the unknown constants k_3 and k_4 . Using the same cases as just used and substituting numerical values into (22) yields:

Case 1: $\mu = 0.5$ for fast cutting, other values as previously given; (22) becomes:

$$k_4 + 14.8 (10^{-3}) k_3 = 1.735 (10^4) \quad (28)$$

Case 2: $\mu = 0.3$ for slow-cutting or a dull wheel, other values as before; (22) becomes:

$$k_4 + 1.06 (10^{-3}) k_3 = 0.182 (10^4) \quad (29)$$

Solving (28) and (29) simultaneously yields the desired constants:

$$k_3^{60} = 1.13 (10^{-6}) \text{ psi}$$

$$k_4^{60} = 630 \text{ psi}$$

Summarizing then, it is found that the constant stresses which exist are:

At the cutting zone:

$$\text{In the normal direction: } k_1^{60} = 2.08 (10^6) \text{ psi}$$

$$\text{In the tangential direction: } k_3^{60} = 1.13 (10^6) \text{ psi}$$

Under the flat on the worn grain:

$$\text{In the normal direction: } k_2^{60} = 3900 \text{ psi}$$

$$\text{In the tangential direction: } k_4^{60} = 630 \text{ psi}$$

2. Tests Using the 90 Grit Wheel

a. Normal Direction: k_1^{90} and k_2^{90} :

In a similar manner (21) will be solved for k_1^{90} and k_2^{90} by using two experimental points from the 90 grit wheel tests.

Case 1: Fast Cutting, high stress condition:

$$\bar{\pi} = 460 \times 10^{-6} \frac{\text{in}}{\text{sec}}; \quad \sigma = 68000 \text{ psi}; \quad F_N = 15 \text{ LB};$$

$$W = .250 \text{ in}; \quad D = 1.75 \text{ in}; \quad D_W = 2.5 \text{ in}; \quad M = 0.167;$$

$$k_g = 2.66 (10^4) \frac{\text{LB}}{\text{IN}}; \quad d = 0.0085 \text{ in}; \quad V = 1340 \frac{\text{in}}{\text{sec}};$$

(21) becomes:

$$k_2 + 15.1 (10^{-3}) k_1 = 2.02 (10^4) \quad (30)$$

Case 2: Slow cutting, low stress condition:

$$\bar{v} = 75 \times 10^{-6} \frac{\text{in}}{\text{sec}}; \quad \sigma = 19300 \text{ psi other values}$$

as above; (21) becomes:

$$k_2 + 1.56 (10^{-3}) k_1 = 0.568 (10^4) \quad (31)$$

Solving (30) and (31) yields the normal-direction constants:

$$k_1^{90} = 1.071 (10^6) \text{ psi}$$

$$k_2^{90} = 4000 \text{ psi}$$

b. Tangential Direction

Solving (22) for the two cases above will yield the unknown constants k_3 and k_4 .

Case 1: As before, fast cutting, so $\mu = 0.5$; (22) becomes:

$$k_4 + 15.1 (10^{-3}) k_3 = 1.01 (10^4) \quad (32)$$

Case 2: Dull wheel, so $\mu = 0.3$; (22) becomes:

$$k_4 + 1.56 (10^{-3}) k_3 = 0.1704 (10^4) \quad (33)$$

Solving (32) and (33) simultaneously yields the tangential-direction constants:

$$k_3^{90} = 0.62 (10^6) \text{ psi}$$

$$k_4^{90} = 750 \text{ psi}$$

Summarizing then for the 90 grit wheel, the constant stresses are found to be:

At the cutting zone:

$$\text{In the normal direction: } k_1^{90} = 1.071 (10^6) \text{ psi}$$

$$\text{In the tangential direction: } k_3^{90} = 0.62 (10^6) \text{ psi}$$

Under the worn grain flat:

$$\text{In the normal direction: } k_2^{90} = 4000 \text{ psi}$$

$$\text{In the tangential direction: } k_4^{90} = 750 \text{ psi}$$

3. Solution of $\left(\frac{\bar{v}}{V}\right)$ Using Constants:

Copying (24) for convenience:

$$\left(\frac{\bar{v}}{V}\right) = \frac{0.106 [dD (mk_g [D_w - D])^5]^{1/2}}{k_1^{3/2} W^{5/4} D_w^{17/12} F_N^{5/12} A_{RL}^{1/4}} \left(F_N - 3.4 k_2 A_{RL}\right)^{3/2}$$

(24 repeated)

Where, as previously noted, the last parenthesis represents the available force for cutting, F_N , minus the force absorbed under the grain flat which will increase as A_{RL} increases. Thus the rate of cutting, \bar{v} , will be diminished as the wheel wears larger flats due to the potential force available being reduced by the force absorbed under the continually growing wear flat area.

The only variable in the above equation, as grinding is begun and continued, for any wheel, is A_{RL} . (F_N is varied independently, for test runs only.) Thus, for the 60 grit wheel tests, the only terms which could vary or be changed were F_N and A_{RL} . The same was true for the 90 grit wheel tests. Then in Appendix 6.1 is given the numerical derivation of the final forms of (24) for the 60 grit wheel. These results are:

$$\bar{v}_{60}^{7.75LB} = \frac{4.0}{\sigma^{5/4}} \left(\frac{\sigma}{k_2^{60}} - 3.4 \right)^{3/2} \quad (34)$$

$$\bar{v}_{60}^{15LB} = \frac{6.91}{\sigma^{5/4}} \left(\frac{\sigma}{k_2^{60}} - 3.4 \right)^{3/2} \quad (35)$$

$$\bar{v}_{60}^{30LB} = \frac{12.3}{\sigma^{5/4}} \left(\frac{\sigma}{k_2^{60}} - 3.4 \right)^{3/2} \quad (36)$$

\bar{v} tabulations for various assumed σ values are given in Table 4 and the theoretical formulas (34), (35), (36) are shown in Figure 12 with the other experimental data for the 60 grit wheel.

In Appendix 6.2 the same is done for the 90 grit wheels. The results are:

$$\bar{v}_{90}^{5LB} = \frac{4.0}{\sigma^{5/4}} \left(\frac{\sigma}{k_2^{90}} - 3.4 \right)^{3/2} \quad (37)$$

$$\bar{v}_{90}^{15LB} = \frac{9.98}{\sigma^{5/4}} \left(\frac{\sigma}{k_2^{90}} - 3.4 \right)^{3/2} \quad (38)$$

$$\bar{v}_{90}^{25LB} = \frac{15.2}{\sigma^{5/4}} \left(\frac{\sigma}{k_2^{90}} - 3.4 \right)^{3/2} \quad (39)$$

\bar{v} tabulations for various assumed σ values are given in Table 5 and the theoretical formulas (37), (38), (39) are shown in Figure 13 with the other experimental data for the 90 grit wheel.

4. $\left(\frac{\bar{v}}{F_N} \right)$ vs. σ As A Linear Function

As stated in the introduction, originally the data obtained was plotted as $\frac{\bar{v}}{F_N}$ vs. σ and a linear relation seemed to exist. Taking equations (34) thru (39) and revising them, using k_2 values, yields:

$$\frac{\bar{v}_{60}^{7.75LB}}{F_N} = \frac{2.1 \times 10^{-6}}{\sigma^{5/4}} \left(\sigma - 13350 \right)^{3/2} \quad (34a)$$

$$\frac{\bar{v}_{60}^{15LB}}{F_N} = \frac{1.87 \times 10^{-6}}{\sigma^{5/4}} \left(\sigma - 13350 \right)^{3/2} \quad (35a)$$

$$\frac{\bar{U}_{60}^{30LB}}{F_N} = \frac{1.67 \times 10^{-6}}{\sigma^{5/4}} (\sigma - 13350)^{3/2} \quad (36a)$$

$$\frac{\bar{U}_{90}^{5LB}}{F_N} = \frac{3.18 \times 10^{-6}}{\sigma^{5/4}} (\sigma - 13400)^{3/2} \quad (37a)$$

$$\frac{\bar{U}_{90}^{15LB}}{F_N} = \frac{2.62 \times 10^{-6}}{\sigma^{5/4}} (\sigma - 13400)^{3/2} \quad (38a)$$

$$\frac{\bar{U}_{90}^{25LB}}{F_N} = \frac{2.4 \times 10^{-6}}{\sigma^{5/4}} (\sigma - 13400)^{3/2} \quad (39a)$$

V Values of these functions are computed for various σ and listed in Table 6. These results are plotted in Figures 14 and 15 with the experimental data.

The approximate linearity of $\left(\frac{\bar{U}}{F_N}\right)$ vs. σ , initially assumed, is easily seen.

F. COMPARISON OF THE CONSTANTS WITH SINGLE
GRAIN SLIDING TESTS

Using the apparatus shown in Figure 16 single grains of aluminum oxide were slid on hardened steel discs (AISI 4150, Rockwell C - 60) at speeds of 3000 - 5000 surface feet-per minute. The results of these tests are shown on Figure 17 along with the results of the conventional grinding tests listed in Tables 1, 2 and 3. (The wheel results have been normalized by considering the fact that a grain in a wheel only contacts the work a fraction of the gross grinding time listed in Tables 1, 2 and 3.) For the condition of stress after 39000 inches of sliding, if it is assumed that after this much sliding, the cutting action has ceased then all the forces (and resulting stresses) measured are from the sliding of the grain flat over the work, then the stresses are measured as:

<u>Distance Slid</u>	<u>σ psi</u>	<u>τ psi</u>
39600 inches	6210	1350
49600 inches	4070	1270

From the analytical work in this paper, the constant stresses determined to exist under the grain flat are:

	60 grit wheel	90 grit wheel
normal direction	$k_2 = 3900$ psi	4000 psi
tangential direction	$k_4 = 630$ psi	750 psi

Comparing these results, the order of magnitudes are correct, and indeed for the longest sliding test, the normal stress measured is almost exactly that derived, 4000 psi.

It is noted in Figure 17 that the continuation of the curve for the wheel tests into the single-grit data is smooth leading to the belief that the wheel merely acts as a group of individual grains and the action of a wheel may be predicted from the behavior of single grains.

This continuation-curve result was the basis for isolating a single grain from the wheel, and assuming a model of stock removal based on the single grain as done in this paper.

G. CONCLUSIONS

Based on single-grain sliding results it was assumed that the action of a grinding wheel could be analyzed by considering a single grain. The grain, with a worn flat, was assumed to have constant stresses acting on it in the normal and tangential directions at the cutting zone where the chip is produced and under the worn flat. The model was analyzed mathematically and the constants found by use of four experimental data points. The sliding constants seemed to agree closely with those found by the single-grain tests. The resulting equations then seemed to predict the results of 57 grinding tests.

Based on these facts the following conclusions may be stated:

1. The cutting potential of a wheel is the normal force and actual stress which it can apply to the work, in the absence of wheel breakage.

2. This normal force available for cutting is gradually reduced by the growth of worn-flat area at the grain-work interface. Since it appears that this junction supports a constant normal stress, the flat area growth gradually absorbs more and more of the available normal force until the area becomes so large it absorbs all the normal force at which time no stock removal would be possible.

3. In the grinding tests conducted the wheel continually removed metal and seemed to reach a situation where $\bar{\sigma}$ was

constant at a low value (about $75 \times 10^{-6} \frac{\text{inch}}{\text{second}}$). The fact that the wheel cutting ability reached a plateau means that the real area of contact, A_{RL} , ceased to grow. Since it was also found that the wheel continually wore down (reaching a low-wear rate plateau at the same time as the low-rate \bar{v} plateau) means that the grains were continually wearing down (at no time did the total wheel wear exceed one grain diameter). Then the only way for the grain to wear down but the area A_{RL} , not to increase must be for some of the area flats to crack out through some mechanism, perhaps thermal. In any one wheel rotation the grain is in contact with the work and absorbs heat, then is plunged into a violently churning coolant bath, possibly causing tensile stresses to develop, causing breakout of the flat area.

4. The above explains why a finely-dressed wheel (diamond dress lead of $50 \times 10^{-6} \frac{\text{inches}}{\text{wheel rev. say}}$) cuts very slowly. A large contact area, A_{RL} is dressed onto the wheel and hence cutting, if possible, is at a slow rate, similar to when a large area has been created by attritious wear.

5. The constant normal and tangential stresses under the grain flats were found to be nearly identical for each wheel (3900 and 630 psi for the 60 grit; 4000 and 750 psi for the 90 grit wheel). Since for the single grit studies values of 4070 and 1270 psi were found for the longest test and since these tests were run dry (no coolant) the use of coolant to reduce sliding friction under the wear flat is questionable in grinding.

6. From well known metal cutting theory see Appendix 7 and Figure 19:

$$\tau_p = k_3 \cos \phi \sin \phi - k_1 \sin^2 \phi$$

Solving this for the 60 and 90 grit constants obtained in this paper, gives:

$$\tau_{\text{plane}} = 140,000 \text{ psi @ } \phi = 14^\circ \text{ for 60 grit}$$

$$\tau_p = 81,000 \text{ psi @ } \phi = 14^\circ \text{ for 90 grit}$$

The work material ground in the tests was AISI 52100 with Rockwell C \sim 60 having a tensile yield strength of about 300,000 psi.

If $\tau_{\text{max}} = \frac{\sigma_y}{2} = 150,000 \text{ psi}$, then the computed results for the 60 grit wheel tests appear to be correct. Why the 90 grit test computation is low is not understood.

7. The constant-stress model thus seems to be valid for the following reasons:

- a. The \bar{v} vs. $\frac{\sigma}{k_2}$ curves shown theoretically and experimentally on Figures 12 and 13 have the proper "shape" and magnitude change with changing F_N .
- b. The values of sliding constants under the grain flat determined from the grinding data and theory give results remarkably similar to single-grit test results after long sliding distances.

- c. For the 60 grit wheel, the constants at the cutting region can be related to the shear strength of the material along an average shear plane. For a shear angle of about 14° it is found that the shear strength is nearly predicted using these constants. If the average grain is assumed to have a zero or negative rake angle, a value of $\phi = 14^\circ$ is reasonable.

APPENDIX

1. Spacing of Effective Grits, \bar{S} :

1.1 Probability of Intersecting

Using Figure 2. Consider a line drawn from the origin "O" in a radial line. The probability of the line intersecting a first-ring grain flat is "P"; the probability of the line getting through or escaping the first ring without intersecting a flat is then (1-P). So that, the following table may be constructed.

Ring No	"P" Hitting Probability	(1-P) Escaping Probability
1	$P_1 = \frac{6\bar{a}}{2\pi L} \frac{(\text{grains})(\text{flat width})}{(\text{circumference of ring})}$	$1 - \frac{6\bar{a}}{2\pi L} = 1 - P_1$
2	$\left(\text{prob. of getting thru 1st ring}\right) \left(\text{prob. of hitting in 2nd ring}\right) = (1-P_1)P_2$ $= (1-P_1) \left[\frac{12\bar{a}}{2\pi(2L)} \right] = (1-P_1)P_1$	$(1-P_1)(1-P_2) = (1-P_1)(1-P_1)$ $= (1-P_1)^2$
23	$(1-P_1)^2 P_3 = (1-P_1)^2 \left[\frac{18\bar{a}}{2\pi(3L)} \right]$ $= (1-P_1)^2 P_1$	$(1-P_1)^2 (1-P_3) = (1-P_1)^2 (1-P_1)$ $= (1-P_1)^3$
k	$P_1 (1-P_1)^{k-1}$	$(1-P_1)^k$

\therefore Probability of the line hitting a flat out to the k^{th} ring =
 $P_1 + P_2 + P_3 + \dots + P_k =$
 $P_1 + (1-P_1)P_1 + (1-P_1)^2 P_1 + \dots + P_1 (1-P_1)^{k-1}$

Probability of still escaping through the k^{th} ring = $(1-P_1)^k$

1.2 Spacing of Effective Grits, \bar{S} :

The average distance travelled along this line is obtained when the probability of intersecting equals the probability of escaping. Thus the escaping probability must be equal 0.5 or:

$$(1 - P_1)^k = 0.5 \quad (1.2.1)$$

$$\begin{aligned} \ln 0.5 &= k \ln (1 - P_1) \\ k &= \frac{\ln 0.5}{\ln (1 - P_1)} \end{aligned} \quad (1.2.2)$$

$$\text{where } P_1 = \frac{3 \bar{a}}{\pi L}$$

Figure 3 is a plot of k vs. P_1 and the curve may be approximated as

$$P_1 k = 1 \quad (1.2.3)$$

$$\text{so that } k = \frac{1}{P_1} = \frac{\pi L}{3 \bar{a}} \quad (1.2.4)$$

Then the average distance travelled by a line from "0" is:

$$\bar{S} = kL \quad (1.2.5)$$

using (1.2.4):

$$\begin{aligned} \bar{S} &= \frac{L}{P_1} \\ \bar{S} &= \pi L^2 / 3 \bar{a} \\ \bar{S} &\approx L^2 / \bar{a} \end{aligned} \quad (1.2.6)$$

2. Length of Contact

2.1 Linearity of Grains in Contact with Length of Contact:

If the array of grinding grits given in Figure 2 is drawn onto a width equal to the workpiece width (i.e. 0.250 inch) and the "S" direction is determined, the resultant picture is given as in Figure 18A. Counting, perpendicular to the \bar{S} direction, the number of grain centerlines intercepted in length $2X = L_c = d$ is found that there are fifty grains intercepted. In a length $2X = 5d$, eighty three centerlines are encountered. Hence the following data may be tabulated:

$2X = L_c$	<u>Number ϕ's Encountered</u>	Ratio $\frac{\text{No } \phi\text{'s Encountered in } L_c}{\text{No } \phi\text{'s Encountered in } L_c = d} = d$	<u>"n"</u>
d	18	1.0	1
2d	35	1.95	2
3d	50	2.78	3
4d	68	3.78	4
5d	83	4.6	5
6d	99	5.5	6
7d	114	6.35	7
8d	132	7.35	8

Then the approximate relationship may be given as:

$$\frac{\text{number of grains in contact for any } L_c = nd}{\text{number of grains in contact for } L_c = d} = n \quad (2.1.1)$$

2.2 Actual Deflection Parallel to F_N : y_{TRUE}

Refer to Figure 18B. For the origin at the wheel centerline (axes $X'y'$), the X, y relation is:

$$X^2 + y^2 = \left(\frac{D}{2}\right)^2$$

moving the coordinates to the rigid-work and wheel interface is accomplished as:

$$X^2 + \left(y - \frac{D}{2}\right)^2 = \left(\frac{D}{2}\right)^2$$

$$X^2 = yD - y^2$$

For small y 's (i.e. $y < .0006$ say), the y^2 term may be neglected, yielding

$$X = \sqrt{yD} \quad (2.2.1)$$

or

$$y = \frac{X^2}{D} \quad (2.2.2)$$

Also from Figure 18B it may be seen that the actual deflected amount of the wheel under some F_N is

$$\begin{aligned} Y_T &= y - y_{WORK} \\ &= \frac{X^2}{D} - \frac{X_W^2}{D_W} \end{aligned}$$

but for small X values, $X = X_W$ so

$$Y_T = \left(\frac{1}{D} - \frac{1}{D_W}\right) X^2$$

$$\text{or } Y_T = \left(\frac{1}{D} - \frac{1}{D_W}\right) \cdot \left(\frac{L_c}{2}\right)^2$$

2.3 Force-Deflection ($F_N - y_T$) or Force-Length of Contact

($F_N - L_c$) Relation:

Now, taking as an assumption that any row of grains may be represented as Figure 18B (i.e. a single grain under a spring,

k_{18})

Then

$$dF_N = k_{18} dy_T \text{ for } 0 < L_c < d$$

and

$$dF_N = 2k_{18} dy_T \text{ for } d < L_c < 2d$$

or generally

$$dF_N = nk_{18} d(y_T) \text{ for } (n-1)d < L_c < nd$$

Thus the force-displacement diagram of Figure 18C may be taken as representing the wheel-work system, for an infinitely-rigid workpiece.

Assume an $F - y_T$ relation as:

$$F_N = B y_T^n \quad (2.3.1)$$

then

$$\frac{dF_N}{dy_T} = Bn (y_T)^{n-1} \quad (2.3.2)$$

The boundary conditions for finding B and n above will vary depending upon "d" (i.e. depending upon the grain size of the wheel being considered).

Then, for the measured data:

$$60 \text{ grit wheel:} \quad 0.044_{\min} < L_c < 0.055_{\max}$$

$$\text{so for } d^{60} = 0.016 \quad 2.75 < L_c < 3.4 \text{ diameters}$$

$$90 \text{ grit wheel:} \quad 0.037_{\min} < L_c < 0.059_{\max}$$

$$\text{so for } d^{90} = 0.0085 \quad 4.3 < L_c < 7 \text{ diameters}$$

Thus the ranges being considered for 60 and 90 grit wheels are shown on Figure 18C.

Then the boundary conditions for (2.3.2) above:

60 grit wheel:

$$(i) \quad \left(\frac{dF}{dy_T} \right) = 3k_{18} \quad @ \quad \frac{y_T}{\left(\frac{1}{D} - \frac{1}{D_w} \right)} = \frac{6.25}{4} d^2 \quad (\text{ie. } L_c = 2.5d)$$

$$(ii) \quad \left(\frac{dF}{dy_T} \right) = 4k_{18} \quad @ \quad \frac{y_T}{\left(\frac{1}{D} - \frac{1}{D_w} \right)} = \frac{12.25}{4} d^2 \quad (\text{ie. } L_c = 3.5d)$$

90 grit wheel:

$$(iii) \quad \left(\frac{dF}{dy_T} \right) = 5k_{18} \quad @ \quad \frac{y_T}{\left(\frac{1}{D} - \frac{1}{D_w} \right)} = \frac{25}{4} d^2 \quad (\text{ie } L_c = 5d)$$

$$(iv) \quad \left(\frac{dF}{dy_T} \right) = 7k_{18} \quad @ \quad \frac{y_T}{\left(\frac{1}{D} - \frac{1}{D_w} \right)} = \frac{49}{4} d^2 \quad (\text{ie } L_c = 7d)$$

Then 60 grit wheel:

$$(i) \quad 3k_{18} = Bn \left[\left(\frac{1}{D} - \frac{1}{D_w} \right) \frac{6.25}{4} d^2 \right]^{n-1}$$

$$(ii) \quad 4k_{18} = Bn \left[\left(\frac{1}{D} - \frac{1}{D_w} \right) \frac{12.25}{4} d^2 \right]^{n-1}$$

Solving (i) for k_1 and inserting it into (ii) yields

$$4 \left\{ \frac{Bn}{3} \left(\left[\frac{1}{D} - \frac{1}{D_w} \right] \frac{6.25}{4} d^2 \right)^{n-1} \right\} = Bn \left\{ \left(\frac{1}{D} - \frac{1}{D_w} \right) \frac{12.25}{4} d^2 \right\}^{n-1}$$

$$\frac{4}{3} (6.25)^{n-1} = (12.25)^{n-1}$$

$$\ln \frac{4}{3} + (n-1) \ln 6.25 = (n-1) \ln 12.25$$

$$0.288 + (n-1) (1.83) = (n-1) (2.5)$$

$$n = 1.4$$

say:

$$n = 1.5$$

Solving for B from (i) using $n = 1.5$ and substituting into (2.3.1) yields

$$F_{N_{60 \text{ grit}}} = 1.6 \left(\frac{k_{60}}{d} \right) \left\{ \left(\frac{DD_w}{D_w - D} \right) \eta_T^3 \right\}^{1/2} \quad (2.3.3)$$

or since

$$\eta_T = \left(\frac{D_w - D}{DD_w} \right) \left(\frac{L_c}{2} \right)^2$$

$$F_{N_{60}} = 1.6 \frac{k_{60}}{d} \left\{ \left(\frac{DD_w}{D_w - D} \right) \left[\left(\frac{D_w - D}{DD_w} \right) \left(\frac{L_c}{2} \right)^2 \right]^3 \right\}^{1/2}$$

$$F_{N_{60}} = 1.6 \frac{k_{60}}{d} \left\{ \left(\frac{D_w - D}{DD_w} \right)^2 \left(\frac{L_c}{2} \right)^6 \right\}^{1/2}$$

$$F_{N_{60}} = 0.2 \frac{k_{60}}{d} \left[\frac{D_w - D}{DD_w} \right] L_c^3$$

(2.3.4)

In a similar manner for the 90 grit wheel:

$$(iii) \quad 5 k_{18} = Bn \left[\left(\frac{1}{D} - \frac{1}{D_w} \right) \frac{25}{4} d^2 \right]^{n-1}$$

$$(iv) \quad 7 k_{18} = Bn \left[\left(\frac{1}{D} - \frac{1}{D_w} \right) \frac{49}{4} d^2 \right]^{n-1}$$

yielding:

$$\frac{7}{5} (25)^{n-1} = (49)^{n-1}$$

$$n = 1.5$$

and as before:

$$F_{N_{90}} = 1.33 \frac{k_{90}}{d} \left[\left(\frac{DD_w}{D_w - D} \right)^{2/2} \gamma_T^3 \right]^{1/2} \quad (2.3.5)$$

or

$$F_{N_{90}} = 0.167 \frac{k_{90}}{d} \left(\frac{D_w - D}{DD_w} \right) L_c^3 \quad (2.3.6)$$

(2.3.4) and (2.3.6) may be written in the form:

$$F_{N_g} = \frac{m_g k_g}{d} \left(\frac{D_w - D}{DD_w} \right) L_c^3 \quad (2.3.7)$$

or

$$L_c = \left[\frac{d D D_w F_N}{m_g k_g (D_w - D)} \right]^{1/3} \quad (2.3.8)$$

2.4 Determination of Spring Constants k_{18}^{60} and k_{18}^{90} :

Obviously k_{18}^{60} and k_{18}^{90} must be determined. For the 60 grit wheel, a measured point was:

$$L_c = 0.047 \text{ inch} @ F_N = 15 \text{ LB}$$

Then this into (2.3.4) using $D_w = 2.37$ inch and $D = 1.87$ inch:

$$15 = \frac{0.2 k_{18}^{60}}{0.016} \left[\frac{2.37 - 1.87}{(2.37)(1.87)} \right] (0.047)^3$$

$$k_{18}^{60} = \frac{15 (0.016) (4.44)}{0.2 (0.5) (104 \times 10^{-6})}$$

$$k_{18}^{60} = 1.025 (10^5) \frac{\text{LB}}{\text{IN}} \quad (2.4.1)$$

For the 90 grit wheel, a measured point was:

$$L_c = 0.005 \text{ inch} @ F_N = 15 \text{ LB}$$

This into (2.3.6) using $D_w = 2.5$ inch and $D = 1.75$ inch:

$$15 = \frac{0.167 k_{18}^{90}}{0.0085} \left[\frac{2.5 - 1.75}{2.5 (1.75)} \right] (0.055)^3$$

$$k_{18}^{90} = \frac{15 (0.0085) (4.37)}{0.167 (0.75) (167 \times 10^{-6})}$$

$$k_{18}^{90} = 2.66 (10^4) \frac{\text{LB}}{\text{IN}} \quad (2.4.2)$$

Inserting these values of k into (2.3.8) using D , D_w , d values as given above, yields

$$L_c^{60} = 0.0192 \sqrt[3]{F_N} \quad (2.4.3)$$

$$L_c^{90} = 0.02 \sqrt[3]{F_N} \quad (2.4.4)$$

Taking an average of these as

$$L_c = 0.0196 F_N^{1/3} \quad (2.4.5)$$

This curve and the remaining experimental data are shown plotted in Figure 18D.

3. General Stress in Normal Direction

Copying (4b):

$$l = \frac{1}{F_N} \left[k_1 b t + k_2 \bar{a}^2 \right]$$

Using (19) and (20) yields

$$1 = \frac{W}{0.294 F_N} \left(\frac{D D_w F_N d}{m k_g d^6 [D_w - D]} \right)^{1/3} \left(0.8 \bar{a} k_1 t + k_2 \bar{a}^2 \right)$$

rewriting:

$$1 = \frac{3.4 W}{F_N^{2/3}} \left[\frac{D D_w d}{m k_g (D_w - D)} \right]^{1/3} \left[0.8 k_1 \left(\frac{\bar{a}}{d} \right) \left(\frac{t}{d} \right) + k_2 \left(\frac{\bar{a}}{d} \right)^2 \right]$$

Using (13a) and (18):

$$1 = \frac{3.4 W}{F_N^{2/3}} \left[\frac{DD_w d}{m k_g (D_w - D)} \right]^{1/3} \left[0.8 k_1 \left(\frac{A_{RL}}{W} \right)^{1/2} \left\{ \frac{m k_g (D_w - D)}{d D D_w F_N} \right\} \frac{1.635}{(Dd)^{2/9}} \cdot \left(\frac{\bar{v}}{V} \right)^{2/3} \left(\frac{W}{A_{RL}} \right)^{1/3} \left\{ \frac{D_w F_N}{m k_g (D_w - D)} \right\}^{1/9} + k_2 \left\{ \frac{A_{RL}}{W} \left(\frac{m k_g [D_w - D]}{d D D_w F_N} \right)^{1/3} \right\} \right]$$

Regrouping:

$$1 = \frac{4.45 k_1 W^{5/6} A_{RL}^{1/6}}{F_N^{13/18}} \left[\frac{1}{m k_g (D_w - D)} \right]^{5/18} (DD_w d)^{3/18} \left(\frac{D_w^7}{D^2 d^2} \right)^{2/18} \left(\frac{\bar{v}}{V} \right)^{2/3} + \frac{3.4 k_2 A_{RL}}{F_N}$$

Using definition of σ , yields:

$$1 = \frac{4.45 k_1 W^{5/6}}{F_N^{5/9} \sigma^{1/6}} \left[\frac{D_w^{17}}{m^5 k_g^5 (D_w - D)^5 (Dd)} \right]^{1/18} \left(\frac{\bar{v}}{V} \right)^{2/3} + 3.4 \frac{k_2}{\sigma}$$

4. General Equation for $\left(\frac{\bar{v}}{V} \right)$:

Copying (23):

$$\left(\frac{\bar{v}}{V} \right)^{2/3} = \left\{ \left[1 - 3.4 \frac{k_2}{\sigma} \right] \left(\frac{\sigma^{1/6} F_N^{5/9}}{4.45 k_1 W^{5/6}} \left[\frac{d D (m k_g [D_w - D])^5}{D_w^{17}} \right]^{1/18} \right) \right\} \quad (4.1.1)$$

$$\left(\frac{\bar{v}}{V} \right) = \frac{\sigma^{1/4} F_N^{15/18}}{9.4 k_1^{3/2} W^{5/4}} \left[\frac{d D (m k_g [D_w - D])^5}{D_w^{17}} \right]^{1/12} \cdot \left(1 - 3.4 \frac{k_2}{\sigma} \right)^{3/2}$$

writing $\sigma = \frac{F_N}{A_{RL}}$ and rearranging the last parenthesis:

$$\left(\frac{\bar{N}}{V}\right) = \frac{0.106}{k_1^{3/2}} \left(\frac{F_N}{A_{RL}}\right)^{1/4} \frac{F_N^{15/8}}{W^{5/4}} \left[\frac{dD (mkg [D_w - D])^5}{D_w^{17}} \right]^{1/2} \cdot \left(\frac{F_N - 3.4 k_2 A_{RL}}{F_N} \right)^{3/2}$$

$$\left(\frac{\bar{N}}{V}\right) = \frac{0.106}{k_1^{3/2} W^{5/4} A_{RL}^{1/4}} F_N^{\frac{9+30-54}{36}} \left[\frac{dD (mkg [D_w - D])^5}{D_w^{17}} \right]^{1/2} \cdot \left(F_N - 3.4 k_2 A_{RL} \right)^{3/2}$$

$$\left(\frac{\bar{N}}{V}\right) = \frac{0.106 [dD (mkg [D_w - D])^5]^{1/2}}{k_1^{3/2} W^{5/4} A_{RL}^{1/4} F_N^{15/36} D_w^{17/12}} \left(F_N - 3.4 k_2 A_{RL} \right)^{3/2}$$

$$\left(\frac{\bar{N}}{V}\right) = \frac{0.106 [dD (mkg [D_w - D])^5]^{1/2}}{k_1^{3/2} W^{5/4} D_w^{17/12} F_N^{5/12} A_{RL}^{1/4}} \left(F_N - 3.4 k_2 A_{RL} \right)^{3/2} \quad (4.1.2)$$

$$\frac{\text{IN}^3 [\text{IN}^2 (\text{LB})^5]^{1/2}}{\text{LB}^{3/2} \text{IN}^{5/4} \text{IN}^{17/12} \text{LB}^{5/12} \text{IN}^{1/2}} (\text{LB})^{3/2} = \frac{\text{LB}^{\frac{5+18}{12} = \frac{23}{12}} \text{IN}^{\frac{36+2}{12} = \frac{38}{12}}}{\text{LB}^{\frac{18+5}{12} = \frac{23}{12}} \text{IN}^{\frac{15+6+17}{12} = \frac{38}{12}}}$$

dimensions check.

5. Scallop-Shaped Assumption

$$\frac{\bar{v}}{V} = \frac{N}{S} \quad (14)$$

Using (20) and (14) yields:

$$\frac{\bar{v}}{V} > \frac{2\sqrt{D}}{d^2/\bar{a}}$$

Using (22)

$$\frac{\bar{v}}{V} > \frac{2D^{1/2}\bar{a}}{d^2} \left[\left(\frac{2\pi D_w \bar{v} d^2}{3 D^{1/2} V \bar{a}} \right)^{2/3} \right]^{1/2}$$

$$\frac{\bar{v}}{V} > \frac{2D^{1/3}\bar{a}^{2/3}}{d^{4/3}} \left(\frac{2\pi}{3} \cdot \frac{D_w \bar{v}}{V} \right)^{1/3}$$

$$\frac{\bar{v}}{V} > 2.56 \left(\frac{DD_w \bar{v}}{V d^2} \right)^{1/3} \left(\frac{\bar{a}}{d} \right)^{2/3}$$

Using (18a)

$$\frac{\bar{v}}{V} > 2.56 \left(\frac{DD_w \bar{v}}{V d^2} \right)^{1/3} \cdot \left\{ \left(\frac{A_{RL}}{W} \right)^{1/2} \cdot \left[\frac{m k_g (D_w - D)}{d D D_w F_N} \right]^{1/6} \right\}^{2/3}$$

$$\frac{\bar{v}}{V} > 2.56 \left(\frac{DD_w \bar{v}}{V d^2} \right)^{1/3} \cdot \left(\frac{A_{RL}}{W} \right)^{1/3} \cdot \left[\frac{m k_g (D_w - D)}{d D D_w F_N} \right]^{1/9}$$

$$\frac{\bar{v}}{V} > 2.56 \left(\frac{D^2 D_w^2}{d^7} \right)^{1/9} \cdot \left(\frac{A_{RL} \bar{v}}{W V} \right)^{1/3} \cdot \left(\frac{m k_g (D_w - D)}{F_N} \right)^{1/9}$$

$$\frac{\bar{v}}{V} > 2.56 \left[\frac{(D D_w)^2 m k_g (D_w - D)}{F_N d^7} \right]^{1/9} \cdot \left[\frac{A_{RL} \bar{v}}{W V} \right]^{1/3}$$

6. Solution of $\left(\frac{\bar{v}}{V}\right)$ Using Constants:

Copying (24):

$$\left(\frac{\bar{v}}{V}\right) = \frac{0.106 [dD(mk_g[D_w-D])^5]^{1/2}}{k_1^{3/2} W^{5/4} D_w^{17/12} F_N^{5/12} A_{RL}^{1/4}} (F_N - 3.4k_2 A_{RL})^{3/2} \quad (24)$$

6.1 60 Grit Wheel Tests:

For the 60 grit wheel the constant terms were as follows:

$$V = 1430 \frac{\text{in}}{\text{sec}}; d = 0.016 \text{ in}; D = 1.87 \text{ in}; M = 0.2; k_g = 1.025 (10^5) \frac{\text{lb}}{\text{in}}$$

$$D_w = 2.37 \text{ in}; k_1 = 2.08 (10^6) \text{ psi}; W = .250 \text{ in}; k_2^{60} = 3900 \text{ psi}.$$

Then insertion of these into (24):

$$\bar{v}_{60 \text{ grit}} = \frac{0.106 (1430) \{0.016 (1.87)\}^{1/2} [0.2 (1.025 \times 10^5) (2.37 - 1.87)]^{5/12}}{(2.08 \times 10^6)^{3/2} (0.250)^{5/4} (2.37)^{17/12} F_N^{5/12} A_{RL}^{1/4}} \cdot (\text{"})^{3/2}$$

$$\bar{v}_{60} = \frac{0.106 (1430) \{0.746\} [47.0]}{(3 \times 10^9) \left(\frac{1}{5.65}\right) (3.4) F_N^{5/12} A_{RL}^{1/4}} (\text{"})^{3/2}$$

$$\bar{v}_{60} = \frac{2.94 \times 10^{-6}}{F_N^{5/12} A_{RL}^{1/4}} [F_N - 3.4k_2 A_{RL}]^{3/2}$$

writing $A_{RL} = F_N/\sigma$ yields:

$$\bar{N}_{60} = \frac{2.94 \times 10^{-6} \sigma^{1/4}}{F_N^{5/12} F_N^{1/4}} \left[F_N - 3.4 k_2 \frac{F_N}{\sigma} \right]^{3/2}$$

$$\bar{N}_{60} = \frac{2.94 \times 10^{-6} \sigma^{1/4} F_N^{3/2}}{F_N^{2/3} \sigma^{3/2}} \left[\sigma - 3.4 k_2 \right]^{3/2} \quad (6.1.1)$$

where the $3.4k_2$ stress is recognized as σ_0 or that stress where $\bar{N} = 0$ as defined previously.

Rearranging:

$$\bar{N}_{60} = \frac{2.94 \times 10^{-6} F_N^{5/6} k_2^{3/2}}{\sigma^{5/4}} \left[\frac{\sigma}{k_2} - 3.4 \right]^{3/2} \quad (6.1.2)$$

Then for tests at various F_N 's:

$$\bar{N}_{60}^{7.75\text{LB}} = \frac{4.0}{\sigma^{5/4}} \left[\frac{\sigma}{k_2^{60}} - 3.4 \right]^{3/2}$$

$$\bar{N}_{60}^{15\text{LB}} = \frac{6.91}{\sigma^{5/4}} \left[\frac{\sigma}{k_2^{60}} - 3.4 \right]^{3/2}$$

$$\bar{N}_{60}^{30\text{LB}} = \frac{12.3}{\sigma^{5/4}} \left[\frac{\sigma}{k_2^{60}} - 3.4 \right]^{3/2}$$

(6.1.3)

6.2. 90 Grit Wheel Tests

For the 90 grit wheel the constant terms were as follows:

$$V = 1340 \frac{\text{in}}{\text{sec}}; d = 0.0085 \text{ in}; D = 1.75 \text{ in}; M = 0.167; k_g = 2.66(10^4);$$

$$D_W = 2.5 \text{ in}; k_1^{90} = 1.071 (10^6) \text{ psi}; W = 1/4 \text{ in}; k_2^{90} = 4000 \text{ psi}.$$

Then insertion of these into (24):

$$\bar{N}_{90} = \frac{0.106 (1340) \{0.0085 (1.75)\}^{1/2} [0.167 (0.266 \times 10^5) (2.5 - 1.75)]^{5/2}}{(1.071 \times 10^6)^{3/2} \left(\frac{1}{4}\right)^{5/4} (2.5)^{7/12} F_N^{5/12} A_{RL}^{1/4}} \left(\text{"}\right)^{3/2}$$

$$\bar{N}_{90} = \frac{0.106 (1340) (0.705) (29.5)}{(1.11 \times 10^9) \left(\frac{1}{5.65}\right) (3.65) F_N^{5/12} A_{RL}^{1/4}} \left(\text{"}\right)^{3/2}$$

$$\bar{N}_{90} = \frac{4.13 \times 10^{-6}}{F_N^{5/12} A_{RL}^{1/4}} \left[F_N - 3.4 k_2 A_{RL} \right]^{3/2}$$

in a manner similar to 6.1, writing $A_{RL} = \frac{F_N}{\sigma}$ yields:

$$\bar{N}_{90} = \frac{4.13 \times 10^{-6} F_N^{5/6} k_2^{3/2}}{\sigma^{5/4}} \left[\frac{\sigma}{k_2} - 3.4 \right]^{3/2} \quad (6.2.2)$$

Then for tests at various F_N 's

$$\bar{N}_{90}^{50} = \frac{4.0}{\sigma^{5/4}} \left[\frac{\sigma}{k_2^{90}} - 3.4 \right]^{3/2}$$

(6.2.3)

$$\bar{\sigma}_{90}^{15LB} = \frac{9.98}{\sigma^{5/4}} \left[\frac{\sigma}{k_2^{90}} - 3.4 \right]^{3/2}$$

$$\bar{\sigma}_{90}^{25LB} = \frac{15.2}{\sigma^{5/4}} \left[\frac{\sigma}{k_2^{90}} - 3.4 \right]^{3/2}$$

(6.2.3 cond't)

7. Metal-Cutting Theory

71.

7.1 Stresses in the Shear Zone:

See Figure 19. From sum of forces along the shear plane direction:

$$k_3^* bt \cos \phi - k_1^* bt \cot \phi \sin \phi = \tau_p \frac{bt}{\sin \phi}$$

$$\tau_p = k_3^* \cos \phi \sin \phi - k_1^* \cos \phi \sin \phi \quad (7.1.1)$$

but the definition of k_3^* and k_1^* used in this paper is

$$k_3 = k_3^*$$

$$k_1 = k_1^* \cot \phi$$

then (7.1.1) becomes

$$\tau_p = k_3 \cos \phi \sin \phi - k_1 \sin^2 \phi \quad (7.1.2)$$

Solving (7.1.2) for $\tau_{p \text{ plane}}$ gives maximum values of:

$$\tau_p^{60} = 140,000 \text{ psi at } \phi = 41.4^\circ$$

$$= 8$$

$$\tau_p^{90} = 81,000 \text{ psi at } \phi = 14^\circ$$

8. Elastic-Rebound Model

8.1 General Equation in Normal Direction

The force equation in the normal direction is:

$$I = \frac{bt}{F_{Ng}} (k_1 + k_2 \bar{a})$$

Using (19) and (20), the above becomes:

$$I = \frac{0.8 \bar{a} t w}{0.294 F_N} \left[\frac{DD_w F_N d}{m k_g (D_w - D) d^6} \right]^{1/3} \cdot \{k_1 + k_2 \bar{a}\}$$

$$I = \frac{2.72 W (\bar{a}/t)}{F_N (d/d)} \left[\frac{DD_w F_N d}{m k_g [D_w - D]} \right]^{1/3} \cdot \{k_1 + k_2 \bar{a}\}$$

using (13a), (13b) and (18):

$$I = \frac{2.72 W}{F_N} \left[\left(\frac{A_{RL}}{W} \right)^{1/2} \cdot \left(\frac{m k_g [D_w - D]}{d D D_w F_N} \right)^{1/6} \right] \cdot \left\{ 1.635 \left(\frac{\bar{r}}{V} \right)^{2/3} \left(\frac{W}{A_{RL}} \right)^{1/3} \left[\frac{D_w^7 F_N}{m k_g (D_w - D) (D d)^2} \right]^{1/9} \right\} \\ \cdot \left(\frac{DD_w F_N d}{m k_g [D_w - D]} \right)^{1/3} \cdot \left\{ k_1 + k_2 \left(\frac{A_{RL}}{W} \right)^{1/2} d \left(\frac{m k_g [D_w - D]}{d D D_w F_N} \right) \right\}$$

combining and using the definition of σ , yields

$$1 = \frac{4.45 W}{F_N^{5/9} \sigma^{1/6}} \left[\left(\frac{\bar{v}}{V} \right)^{2/3} \cdot \left\{ \frac{D_w}{m k_g (D_w - D)} \right\}^{5/18} \left(\frac{D_w^{12}}{d D} \right)^{1/18} \right] \left\{ k_1 + \frac{k_2 F_N^{1/3} d}{(\sigma W)^{1/2}} \left[\frac{m k_g [D_w - D]}{d D D_w} \right] \right\}^{1/6}$$

(8.1.1)

8.2 Solution in Normal Direction Using Data Points

The solution of this model using the cases already described yields the following equations:

$$k_1^{60} + 1.129 (10^{-3}) k_2^{60} = 232 (10^4)$$

Slow cutting:

$$k_1^{60} + 2.69 (10^{-3}) k_2^{60} = 566 (10^4)$$

Solving these simultaneously yields:

$$k_2^{60} = -10^5 \text{ psi}$$

$$k_2^{60} = 214 (10^7) \frac{\text{lb}}{\text{in}^3}$$

These results dictate that the normal stress applied by the grain on the work in the cutting region is tensile so as to compensate for the stress under the grain flat which is very large. This model is thus discarded.

SERIES NO	F_N (LB)	\bar{v} ($\frac{\text{INCH} \times 10^{-6}}{\text{SECOND}}$)	A_{RL} ($\text{IN}^2 \times 10^{-6}$)	$\frac{\bar{v}}{F_N}$ ($\frac{\text{IN} \times 10^{-6}}{\text{SEC, LB}}$)	σ ($\frac{\text{LB}}{\text{IN}^2}$)	$\frac{\sigma}{k_2}$	TIME OF GRINDING & SINCE t=0 (SECONDS)
1	15	75	758	5.0	19,784	5.08	760
2	15	75	660	5.0	22,730	5.82	760
3	15	75	774	5.0	19,374	4.97	760
4	15	440	121	29.4	123,920	31.8	13
5	15	440	131	29.4	113,745	29.2	13
6	15	275	272	18.35	55,152	14.1	44
7	15	275	285	18.35	52,542	13.45	44
8	15	155	451	10.35	33,253	8.51	91
9	15	155	326	10.35	45,960	11.8	91
10	7.75	55	327	7.1	23,653	6.05	371
11	7.75	55	377	7.1	20,760	5.3	371
12	7.75	280	69	36.2	111,727	28.6	20
13	7.75	280	87	36.2	89,356	22.9	20
14	7.75	150	210	19.35	36,991	9.5	96
15	7.75	150	148	19.35	52,333	13.4	96
16	30	110	1664	3.67	18,022	4.61	430
17	30	110	1472	3.67	20,377	5.21	430
18	30	360	730	12.0	41,095	10.5	149
19	30	360	684	12.0	43,861	11.2	149
20	30	200	677	6.67	44,315	11.35	148
21	30	590	534	19.7	56,195	14.4	42

(60 GRIT WHEEL)
TABLE 1

SERIES No	F_N (LB)	\bar{v} (MICROINCH SECOND)	A_{RL} ($IN^2 \times 10^{-6}$)	$\frac{\bar{v}}{F_N}$ ($\frac{IN \times 10^{-6}}{SEC, LB}$)	σ ($\frac{LB}{IN^2}$)	$\frac{\sigma}{k_2}$	TIME OF GRINDING SINCE $t=0$ (SECONDS)
22	5	25	119	5.0	41,986	10.5	450
23	5	25	283	5.0	17,698	4.44	450
24	5	25	220	5.0	22,688	5.67	388
25	5	25	247	5.0	20,240	5.07	388
26	5	95	74	19.0	67,615	16.9	42
27	5	95	129	19.0	38753	9.68	42
28	5	150	63	30.0	79,353	19.8	20
29	5	150	78	30.0	63,763	15.9	20
30	15	75	777	5.0	19,309	4.83	490
31	15	75	1062	5.0	14,125	3.53	490
32	15	50	884	3.33	16,970	4.25	470
33	15	50	958	3.33	15,665	3.92	470
34	15	230	661	15.3	22,691	5.67	136
35	15	230	611	15.3	24,558	6.15	136
36	15	320	293	21.4	51,115	12.8	52
37	15	320	406	21.4	36,975	9.25	52
38	15	550	108	36.7	139,346	9.85	13
39	15	550	219	36.7	68,466	17.1	13
40	15	460	255	30.7	58,736	14.7	24
41	15	460	191	30.7	78,740	19.7	24
42	15	290	446	19.3	33,633	8.4	78

(90 GRIT WHEEL)

TABLE 2

SERIES NO	F_N (LB)	\bar{v} (INCH $\times 10^{-6}$) SECOND)	A_{RL} (IN $^2 \times 10^{-6}$)	$\frac{\bar{v}}{F_N}$ (IN $\times 10^{-6}$) SEC, LB)	σ ($\frac{LB}{IN^2}$)	$\frac{\sigma}{K_2}$	TIME OF GRINDING SINCE $t=0$ (SECONDS)
43	15	290	793	19.3	18,917	4.73	78
44	25	70	1442	2.8	17,333	4.33	316
45	25	70	1620	2.8	15,431	3.85	316
46	25	70	1984	2.8	12,600	3.25	360
47	25	70	1683	2.8	14,853	3.71	360
48	25	270	1060	10.8	23,591	5.9	43
49	25	270	775	10.8	32,242	8.05	43
50	25	510	567	20.4	44,084	11.0	27
51	25	510	371	20.4	67,470	16.9	27
52	25	350	1176	14.0	21,237	5.3	67
53	25	350	1193	14.0	20,948	5.25	67
54	25	480	1242	19.2	20,125	5.05	28
55	25	480	1181	19.2	21,165	5.27	28
56	25	180	1705	7.2	14,658	3.69	124
57	25	180	1217	7.2	20,550	5.14	124

(90 GRIT WHEEL)

TABLE 3

σ (psi)	$\frac{1}{\sigma^{5/4}}$	$\frac{\sigma}{k_2^{60}}$	$\left(\frac{\sigma}{k_2^{60}} - 3.4\right)$	$\left(\frac{\sigma}{k_2^{60}} - 3.4\right)^{1.5}$	$\frac{\left(\frac{\sigma}{k_2^{60}} - 3.4\right)^{3/2}}{\sigma^{5/4}}$	$\bar{N}_{7.75}$ $\left(\frac{IN \times 10^{-6}}{SEC.}\right)$	\bar{N}_{15} $\left(\frac{IN \times 10^{-6}}{SEC.}\right)$	\bar{N}_{30} $\left(\frac{IN \times 10^{-6}}{SEC.}\right)$
$2(10^4)$	$4.2(10^{-6})$	5.13	1.73	2.28	$9.56(10^{-6})$	38.3	66.0	118.0
$4(10^4)$	$1.77(10^{-6})$	10.25	6.85	18.0	$31.9(10^{-6})$	128	220	392
$6(10^4)$	$1.062(10^{-6})$	15.4	12.0	41.7	$44.4(10^{-6})$	177	306	545
$8(10^4)$	$0.74(10^{-6})$	20.5	17.1	71.0	$52.5(10^{-6})$	210	363	645
10^5	$0.564(10^{-6})$	25.6	22.2	105.0	$59.1(10^{-6})$	236	410	725
$1.3(10^5)$	$0.405(10^{-6})$	33.3	29.9	166.0	$67.3(10^{-6})$	270	465	830

FORMULAS FROM TEXT:

$$\bar{N}_{7.75LB} = \frac{4.0}{\sigma^{5/4}} \left\{ \frac{\sigma}{k_2^{60}} - 3.4 \right\}^{3/2} \dots \dots (34)$$

$$\bar{N}_{15LB} = \frac{6.91}{\sigma^{5/4}} \left\{ \frac{\sigma}{k_2^{60}} - 3.4 \right\}^{3/2} \dots \dots (35)$$

$$\bar{N}_{30LB} = \frac{12.3}{\sigma^{5/4}} \left\{ \frac{\sigma}{k_2^{60}} - 3.4 \right\}^{3/2} \dots \dots (36)$$

WHERE: $k_2^{60} = 3900$ psi

(60 GRIT WHEEL)
TABLE 4

σ (psi)	$\frac{1}{\sigma^{5/4}}$	$\frac{\sigma}{k_2^{90}}$	$\left(\frac{\sigma}{k_2^{90}} - 3.4\right)$	$\left(\frac{\sigma}{k_2^{90}} - 3.4\right)^{3/2}$	$\frac{\left(\frac{\sigma}{k_2^{90}} - 3.4\right)^{3/2}}{\sigma^{5/4}}$	\bar{N}_5 $\left(\frac{IN \times 10^{-6}}{SEC}\right)$	\bar{N}_{15} $\left(\frac{IN \times 10^{-6}}{SEC.}\right)$	\bar{N}_{25} $\left(\frac{IN \times 10^{-6}}{SEC.}\right)$
$2(10^4)$	$4.2(10^{-6})$	5.0	1.6	2.04	$8.57(10^{-6})$	34	85	130
$4(10^4)$	$1.77(10^{-6})$	10.0	6.6	17.0	$30.1(10^{-6})$	120	300	458
$6(10^4)$	$1.062(10^{-6})$	15.0	11.6	40	$42.6(10^{-6})$	170	425	650
$8(10^4)$	$0.74(10^{-6})$	20.0	16.6	68	$50.4(10^{-6})$	200	500	765
10^5	$0.564(10^{-6})$	25.0	21.6	100	$56.4(10^{-6})$	226	560	855
$1.3(10^5)$	$0.405(10^{-6})$	32.5	29.1	159	$64.4(10^{-6})$	258	640	980

FORMULAS FROM THE TEXT:

$$\bar{N}_{5lb} = \frac{4.0}{\sigma^{5/4}} \left\{ \frac{\sigma}{k_2^{90}} - 3.4 \right\}^{3/2} \dots \dots \dots (37)$$

$$\bar{N}_{15lb} = \frac{9.98}{\sigma^{5/4}} \left\{ \frac{\sigma}{k_2^{90}} - 3.4 \right\}^{3/2} \dots \dots \dots (38)$$

$$\bar{N}_{25lb} = \frac{15.2}{\sigma^{5/4}} \left\{ \frac{\sigma}{k_2^{90}} - 3.4 \right\}^{3/2} \dots \dots \dots (39)$$

WHERE: $k_2^{90} = 4000$ psi

(90 GRIT WHEEL)
TABLE 5

σ (psi)	$\frac{(\sigma - 3.4 \times 10^4)^{3/2}}{\sigma^{5/4}}$	$\left(\frac{\bar{v}}{F_N}\right)^{LB} \left(\frac{IN \times 10^{-6}}{SEC, LB}\right)$ 7.75 LB ~ 60 GRIT 5.0 LB ~ 90 GRIT	$\left(\frac{\bar{v}}{F_N}\right)^{LB} \left(\frac{IN \times 10^{-6}}{SEC, LB}\right)$ 15 LB ~ 60 GRIT 90 GRIT	$\left(\frac{\bar{v}}{F_N}\right)^{LB} \left(\frac{IN \times 10^{-6}}{SEC, LB}\right)$ 30 LB ~ 60 GRIT 25 LB ~ 90 GRIT
-------------------	---	---	--	--

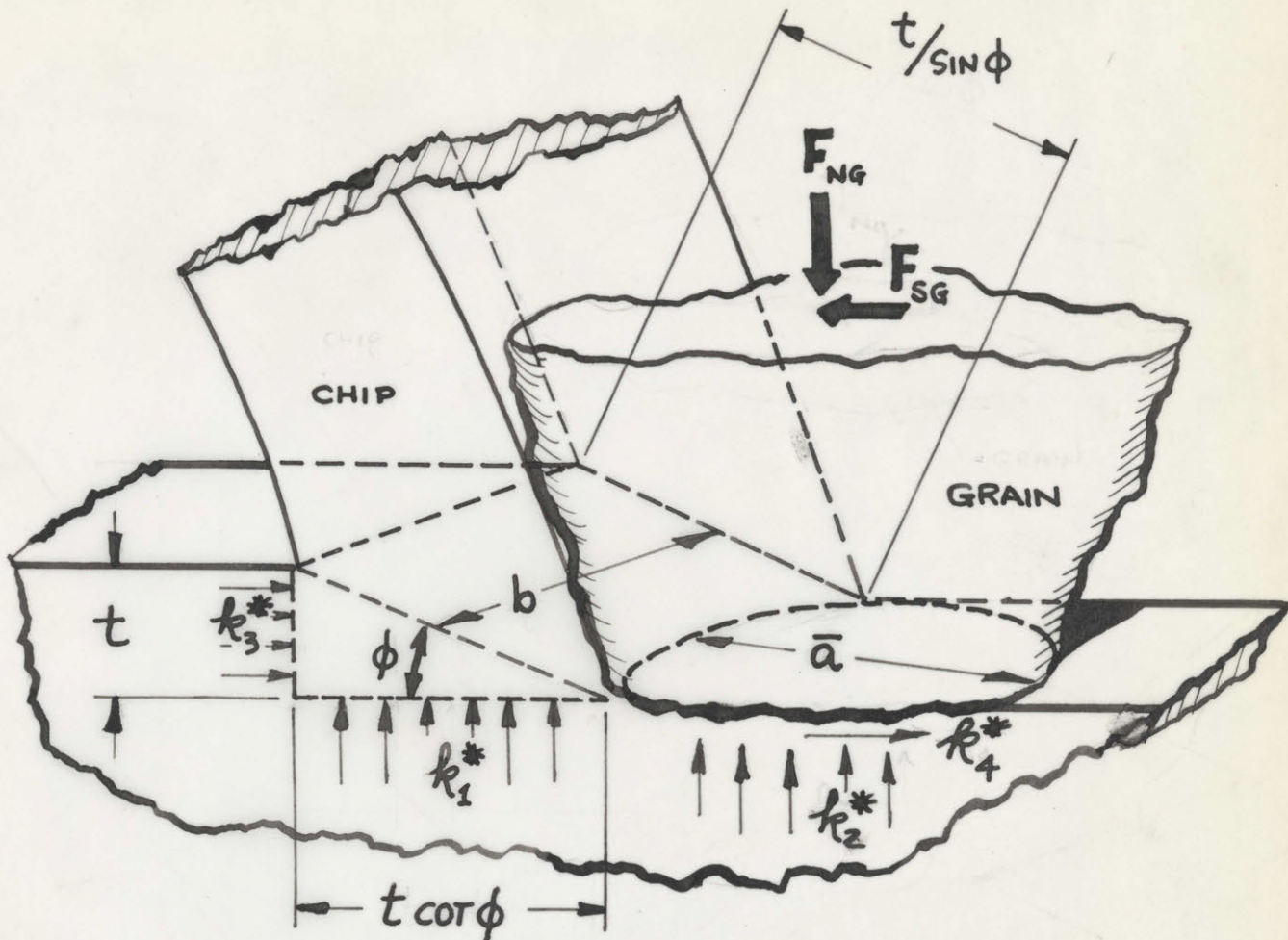
60 GRIT WHEEL

$2(10^4)$	2.28	$\left(\frac{\bar{v}}{F_N}\right)^{7.75LB} = 4.8$	$\left(\frac{\bar{v}}{F_N}\right)^{15LB} = 4.28$	$\left(\frac{\bar{v}}{F_N}\right)^{30LB} = 3.81$
$4(10^4)$	7.7	16.2	14.4	12.9
$6(10^4)$	10.75	22.6	20.1	18.0
$8(10^4)$	12.71	26.8	23.8	21.3
10^5	14.4	30.2	27.0	24.0
$1.3(10^5)$	16.2	34.0	30.4	27.1

90 GRIT WHEEL

$2(10^4)$	2.28	$\left(\frac{\bar{v}}{F_N}\right)^{5LB} = 7.25$	$\left(\frac{\bar{v}}{F_N}\right)^{15LB} = 5.0$	$\left(\frac{\bar{v}}{F_N}\right)^{25LB} = 5.47$
$4(10^4)$	7.7	24.5	20.2	18.5
$6(10^4)$	10.75	34.2	28.2	25.8
$8(10^4)$	12.71	40.5	33.4	30.6
10^5	14.4	45.8	37.7	34.6
$1.3(10^5)$	16.2	51.5	42.5	39.0

TABLE 6



FOR ELASTIC-REBOUND MODEL:

AT THE SHEAR ZONE:

$$F_V = k_1^* b t \cot\phi$$

$$F_H = k_3^* b t$$

AT THE SLIDING ZONE:

$$F_V = k_2^* \bar{a} b t$$

$$F_H = k_4^* \bar{a} b t$$

FOR CONSTANT-STRESS MODEL:

AT THE SHEAR ZONE:

$$F_V = k_1^* b t \cot\phi$$

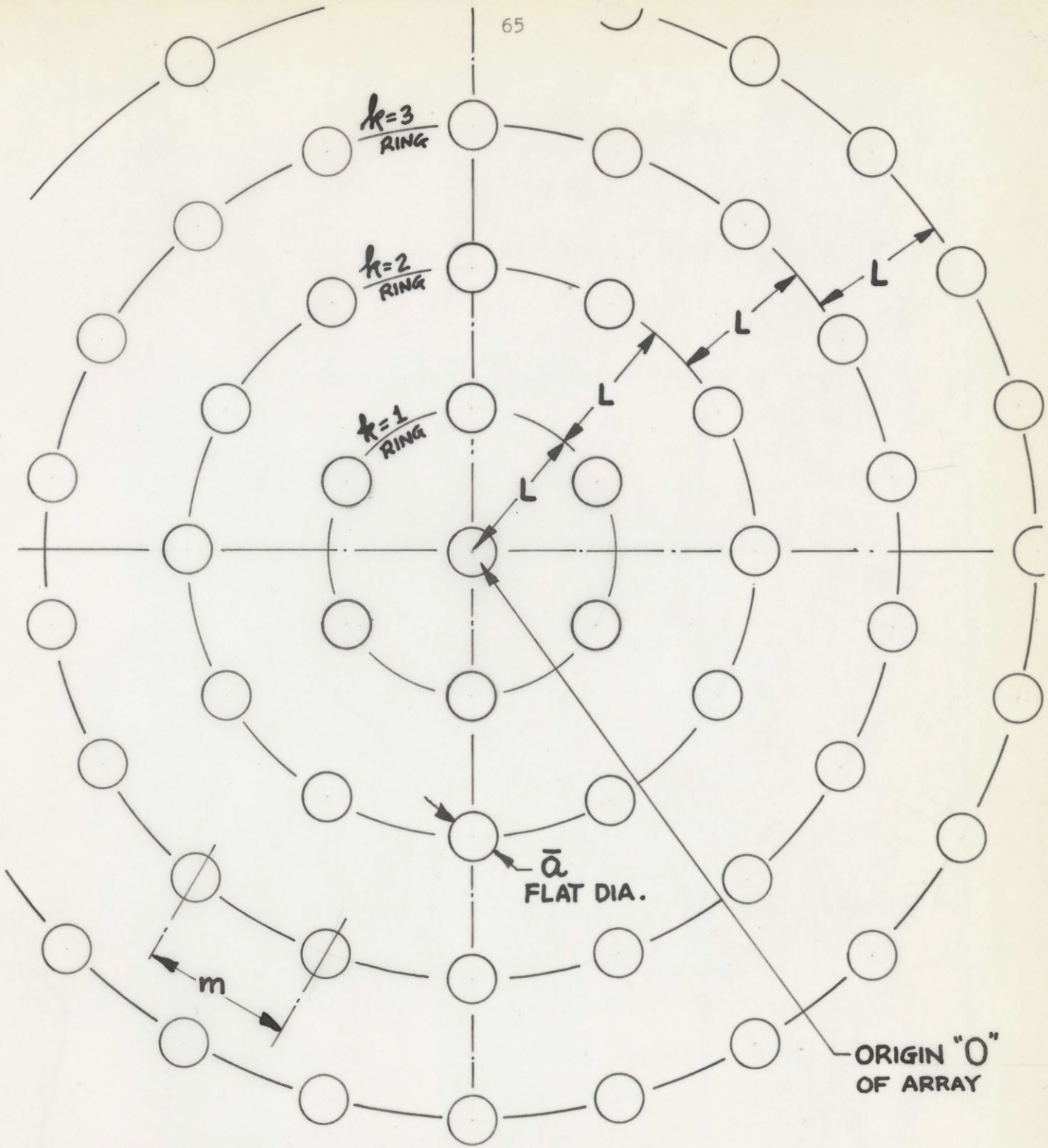
$$F_H = k_3^* b t$$

AT THE SLIDING ZONE:

$$F_V = k_2^* \left(\frac{\pi \bar{a}^2}{4} \right)$$

$$F_H = k_4^* \left(\frac{\pi \bar{a}^2}{4} \right)$$

FIG. 1 GRAIN-CHIP GEOMETRY



NUMBER OF GRAINS IN ANY RING = $6k$
 WHERE k IS NUMBER OF RING

$$m = \frac{2\pi R}{N^{\circ} \text{GRAINS}} = \frac{2\pi(kL)}{6k}$$

$\therefore m = \frac{\pi L}{3}$ INDEPENDENT OF RING NUMBER

FIG. 2 ARRAY OF GRAINS

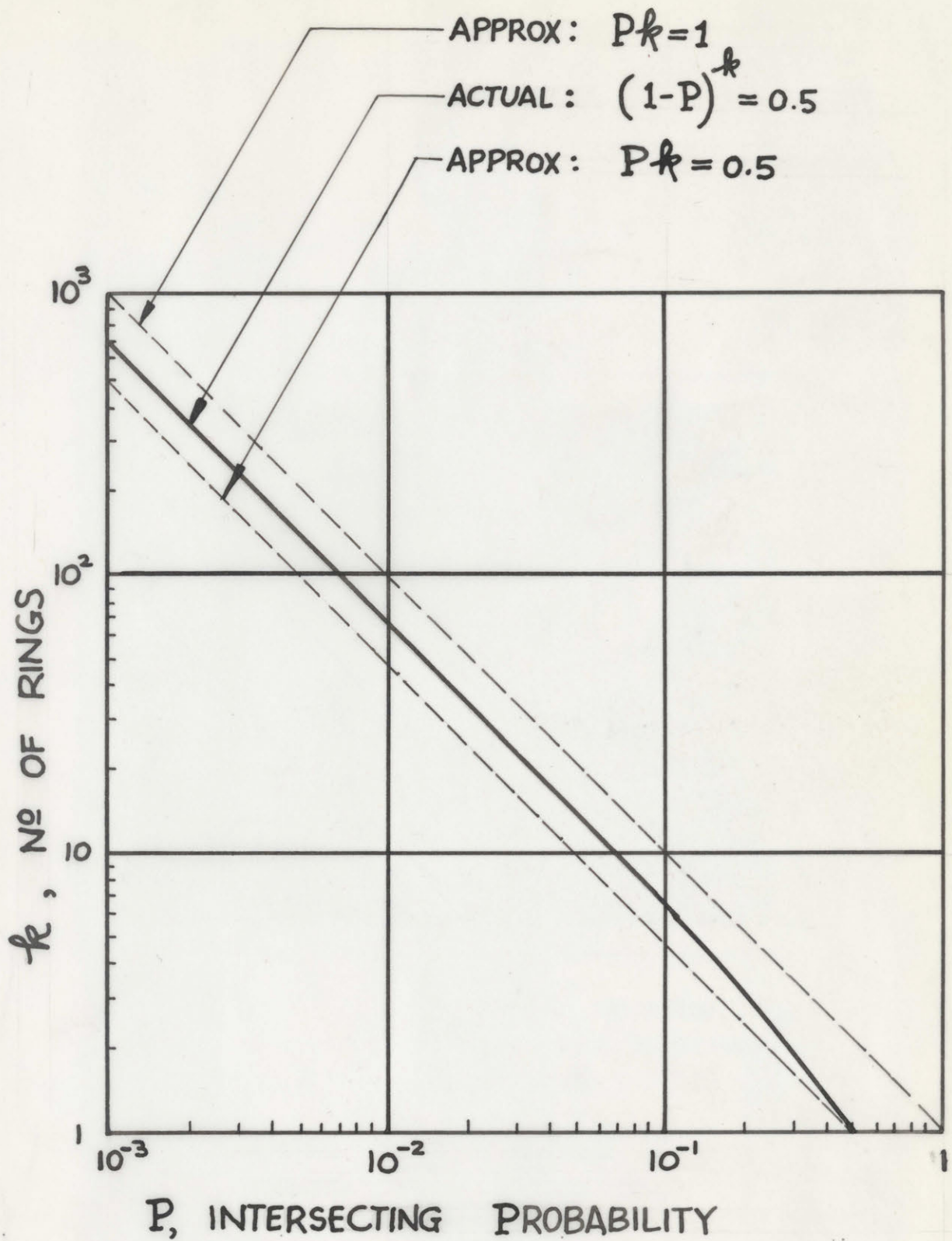
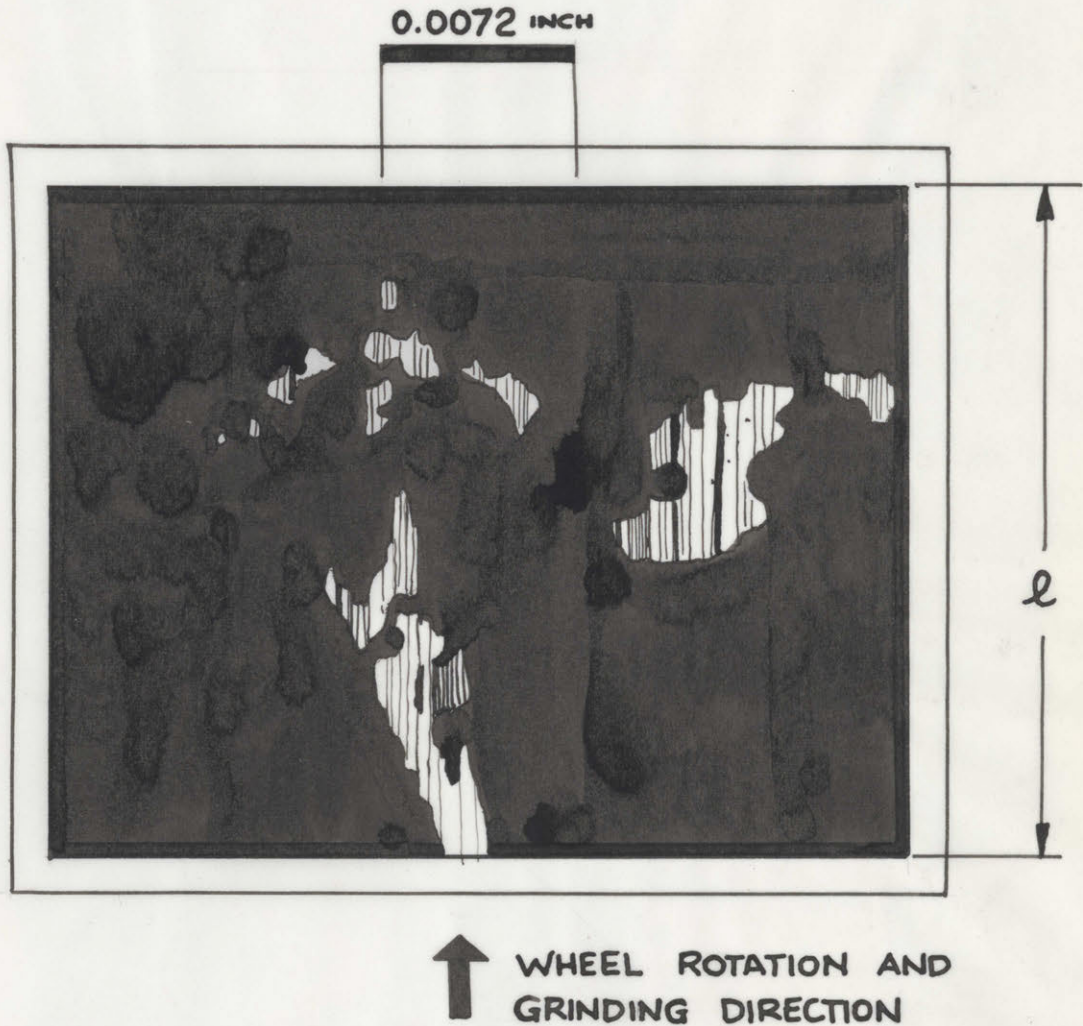


FIG. 3

 k vs. P



(ABOVE IS A DRAWING
TRACED FROM AN ACTUAL
PHOTOGRAPH)

FIG. 4 PHOTO OF WORN WHEEL

STRIP REPRESENTS 0.250 INCH ACTUAL WIDTH OF WORKPIECE



SERIES N^o 21 : $\bar{v} = 590 \times 10^{-6} \frac{\text{INCH}}{\text{SEC}}$; $F_N = 30 \text{ LB}$; $A_{RL} = 534 \times 10^{-6} \text{ INCH}^2$; $\sigma = 56,195 \text{ psi}$

$l = 0.025 \text{ INCH}$



SERIES N^o 19 : $\bar{v} = 360 \times 10^{-6} \frac{\text{INCH}}{\text{SEC}}$; $F_N = 30 \text{ LB}$; $A_{RL} = 684 \times 10^{-6} \text{ IN}^2$; $\sigma = 43,861 \text{ psi}$



SERIES N^o 17 : $\bar{v} = 110 \times 10^{-6} \frac{\text{INCH}}{\text{SEC}}$; $F_N = 30 \text{ LB}$; $A_{RL} = 1472 \times 10^{-6} \text{ IN}^2$; $\sigma = 20,377 \text{ psi}$

ABOVE DRAWINGS WERE TRACED FROM ACTUAL PHOTOGRAPHIC "STRIPS". ORIGINAL STRIPS WERE REDUCED IN SIZE.

FIG. 5 PHOTO "STRIPS" OF THREE WORN WHEELS

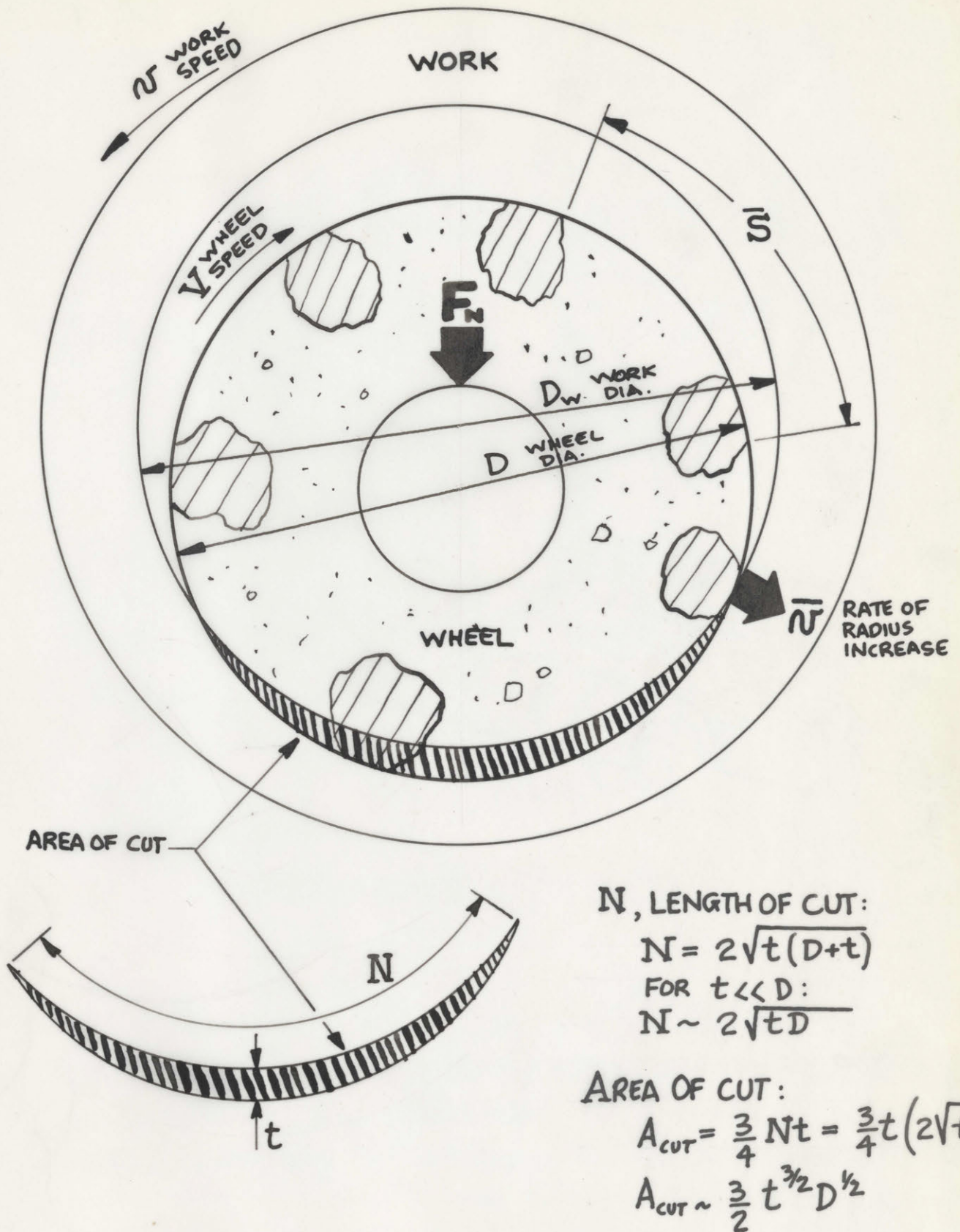


FIG.6 CUTTING GEOMETRY

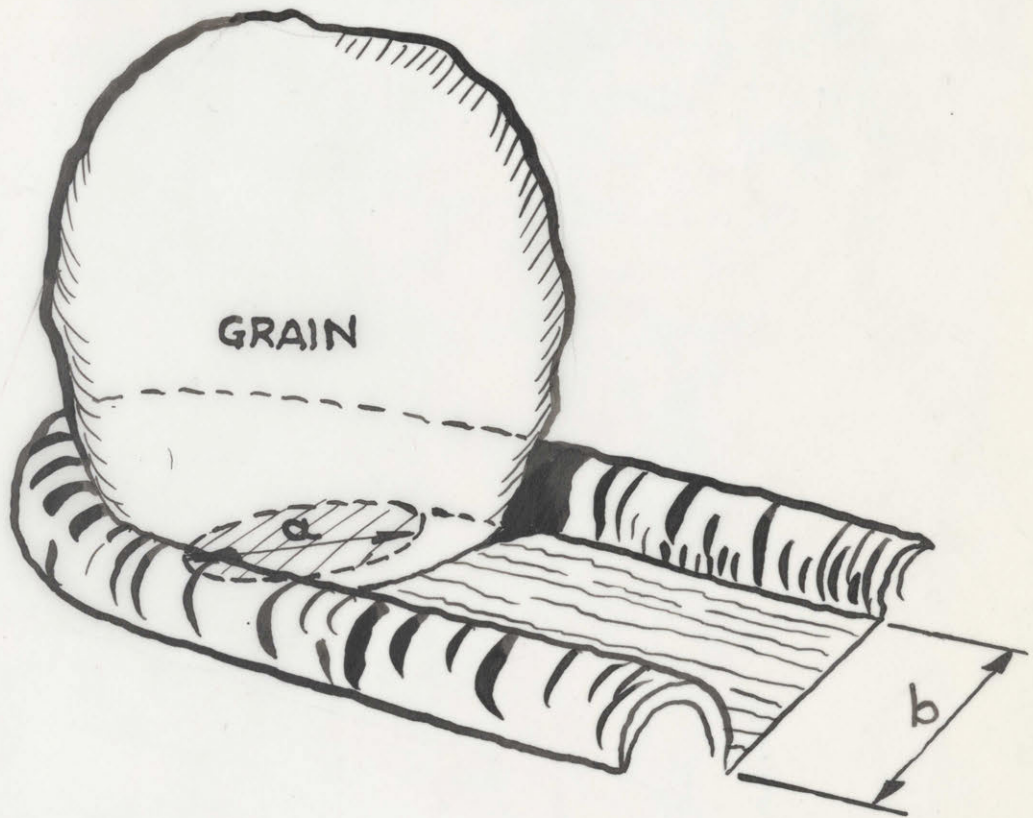
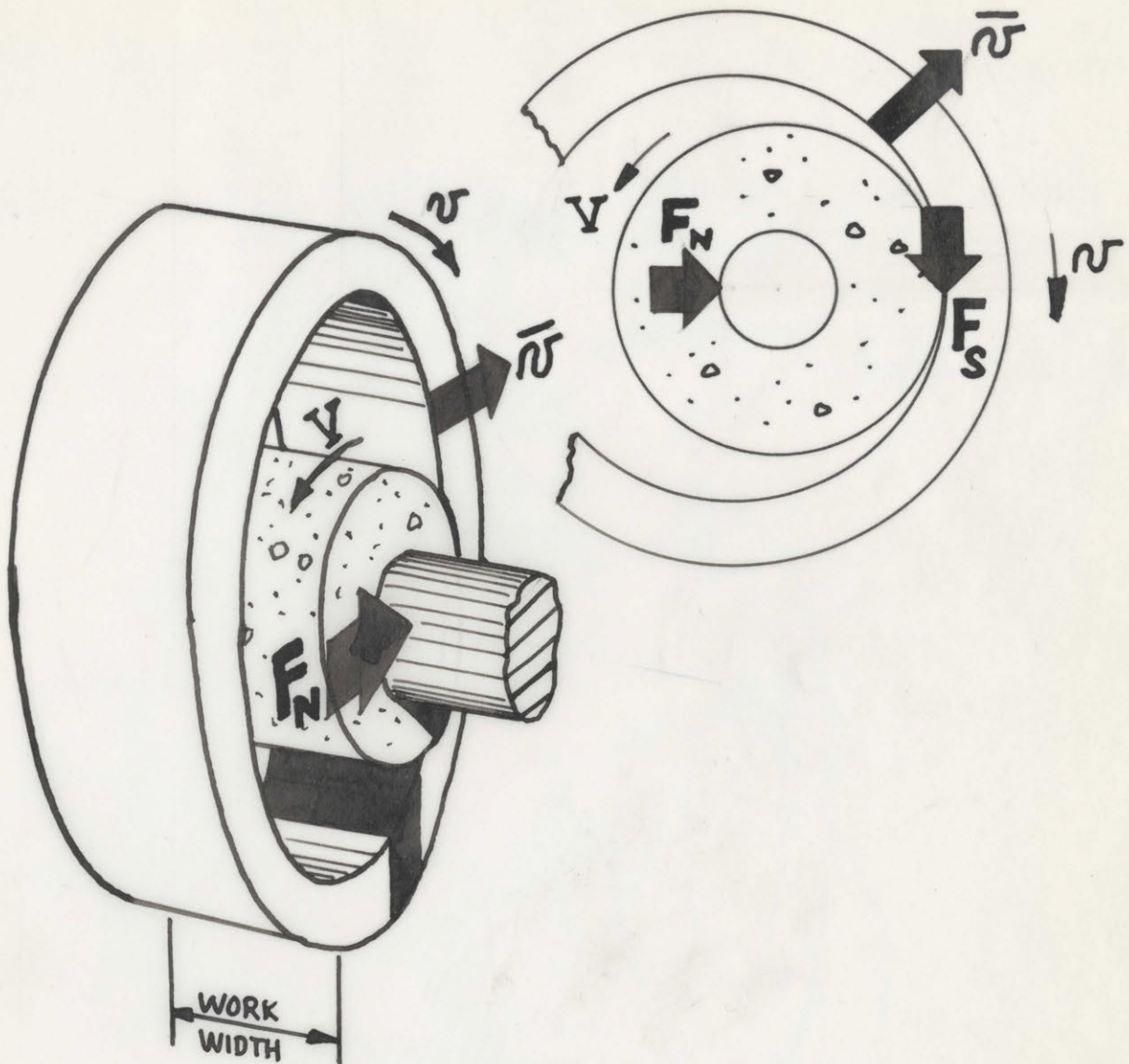


FIG. 7 WIDTH OF CUT, b



EXPERIMENTAL DATA

$$\mu_{\text{SHARP WHEEL}} = \frac{F_S}{F_N} = 0.5$$

$$\mu_{\text{DULL WHEEL}} = 0.3$$

WORK MATERIAL: AISI-E52100 @ ROCKWELL C~62

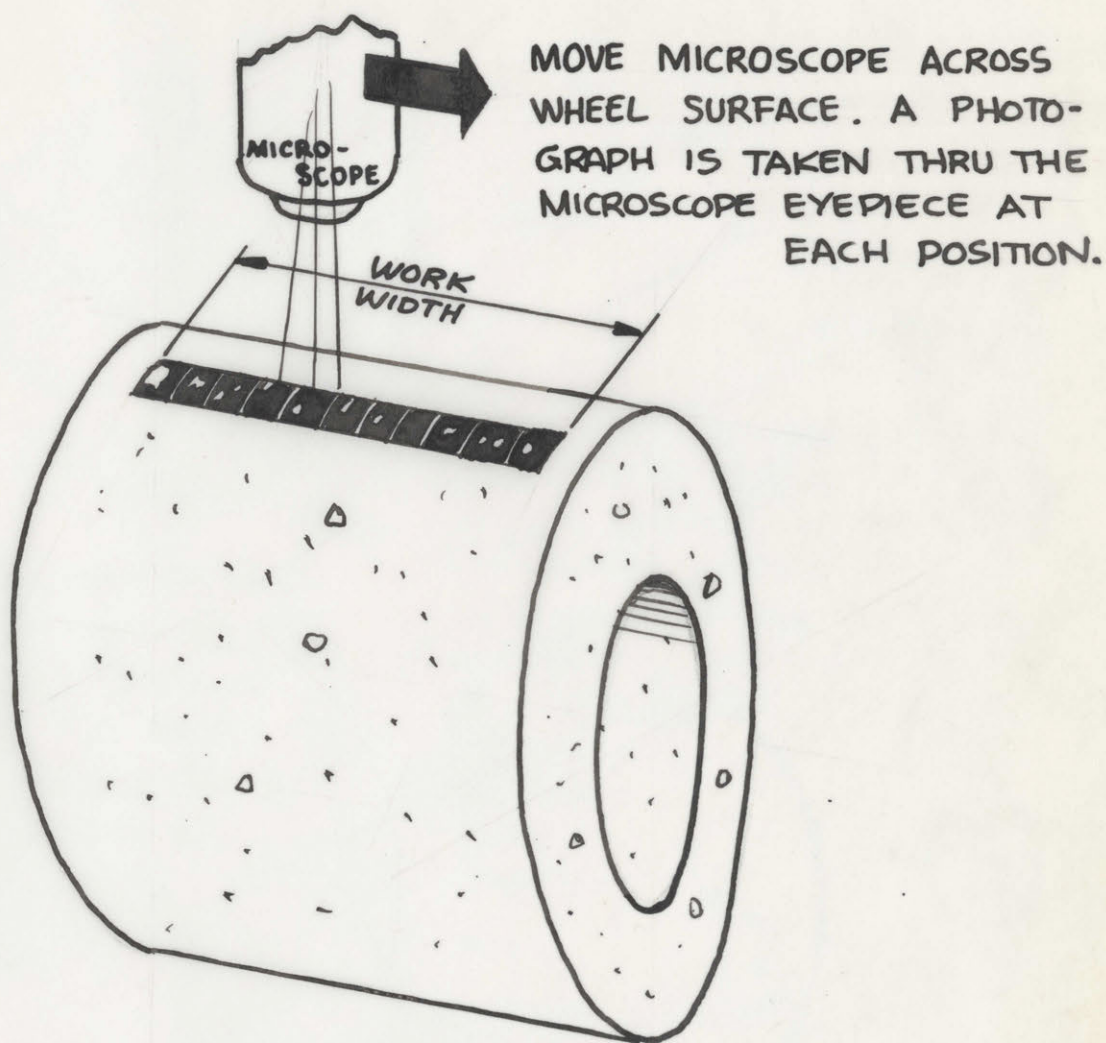
WORK WIDTH, $W \equiv 0.250$ INCH

WORK DIAMETER: $\sim 2\frac{3}{8}$ DIA. FOR 60 GRIT WHEEL TESTS
 $\sim 2\frac{1}{2}$ INCH DIA. FOR 90 GRIT WHEEL

WHEEL DATA: A60L5V NORTON, $1\frac{7}{8}$ DIA \times $\frac{3}{8}$ WIDE \times 14600 rpm
 2A90P6 CINCINNATI, $1\frac{3}{4}$ DIA \times $\frac{3}{8}$ WIDE \times 14600 rpm

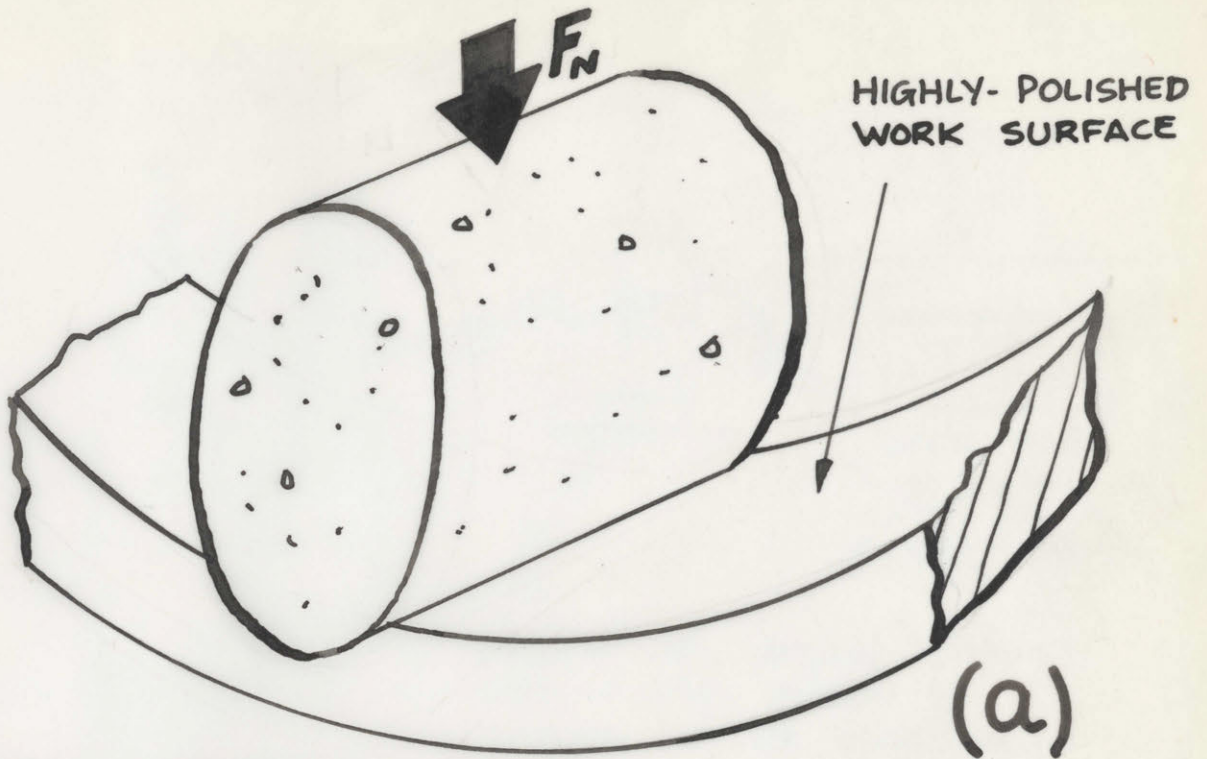
COOLANT: TEXACO "SOLUBLE D" PLUNGE GRINDING ONLY

FIG. 8 EXPERIMENTAL DATA

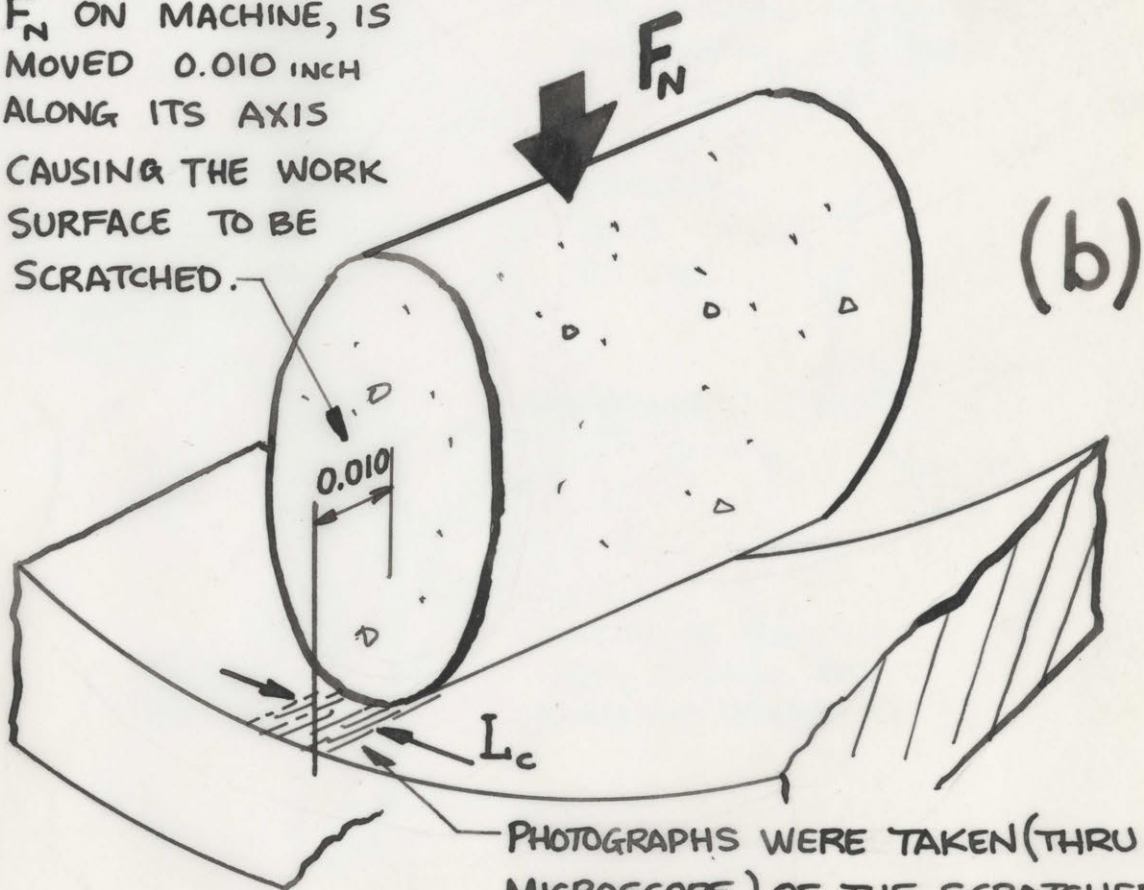


WORK WIDTH WAS 0.250 INCH ; WHEELS WERE $\frac{3}{8}$ INCH WIDE , AND SINCE ONLY PLUNGE GRINDING WAS PERFORMED, THE WORN PORTION OF THE WHEEL WAS EASILY DISCERNABLE

FIG. 9 OBTAINING A "STRIP"

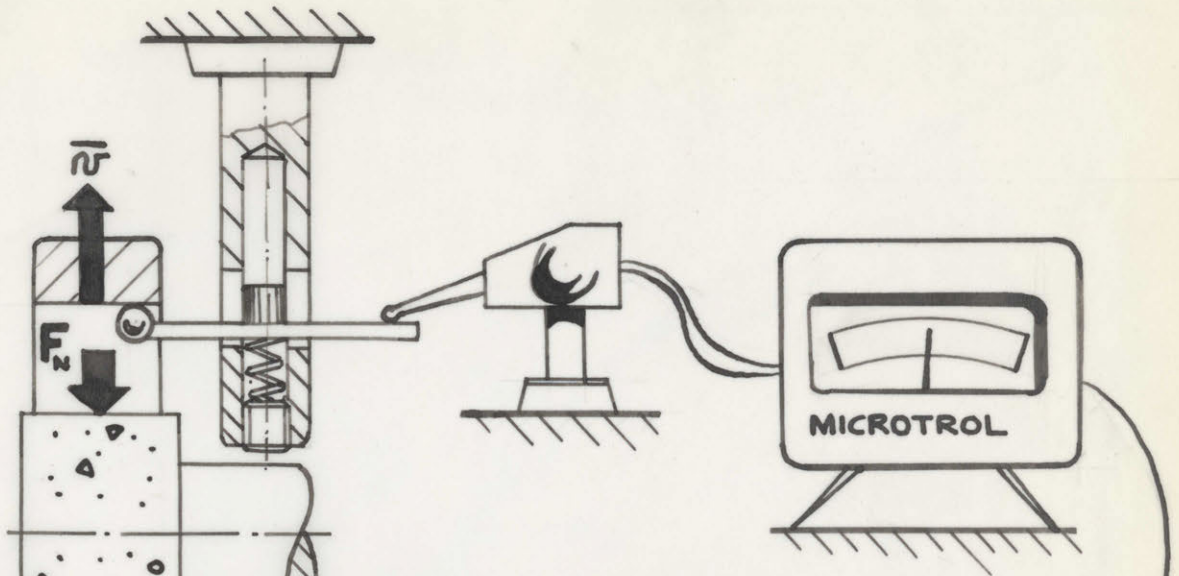


WHEEL, LOADED WITH F_N ON MACHINE, IS MOVED 0.010 INCH ALONG ITS AXIS CAUSING THE WORK SURFACE TO BE SCRATCHED.



PHOTOGRAPHS WERE TAKEN (THRU A MICROSCOPE) OF THE SCRATCHED WORK. THE AVERAGE WIDTH OF THE BAND (ABOUT 30 READINGS WERE TAKEN) WAS DESIGNATED L_c , LENGTH OF CONTACT

FIG. 10 OBTAINING L_c



MOTION OF SPRING-LOADED, WORK-RIDING PROBE IS PICKED UP BY MICROTRON ELECTRONIC INDICATOR.

THE SIGNAL FROM THE MICROTRON IS FED TO A RECORDER,

GIVING A POSITION-TIME GRAPH.

FREE MOTION OF MACHINE XSLIDE UNTIL WHEEL-WORK CONTACT.

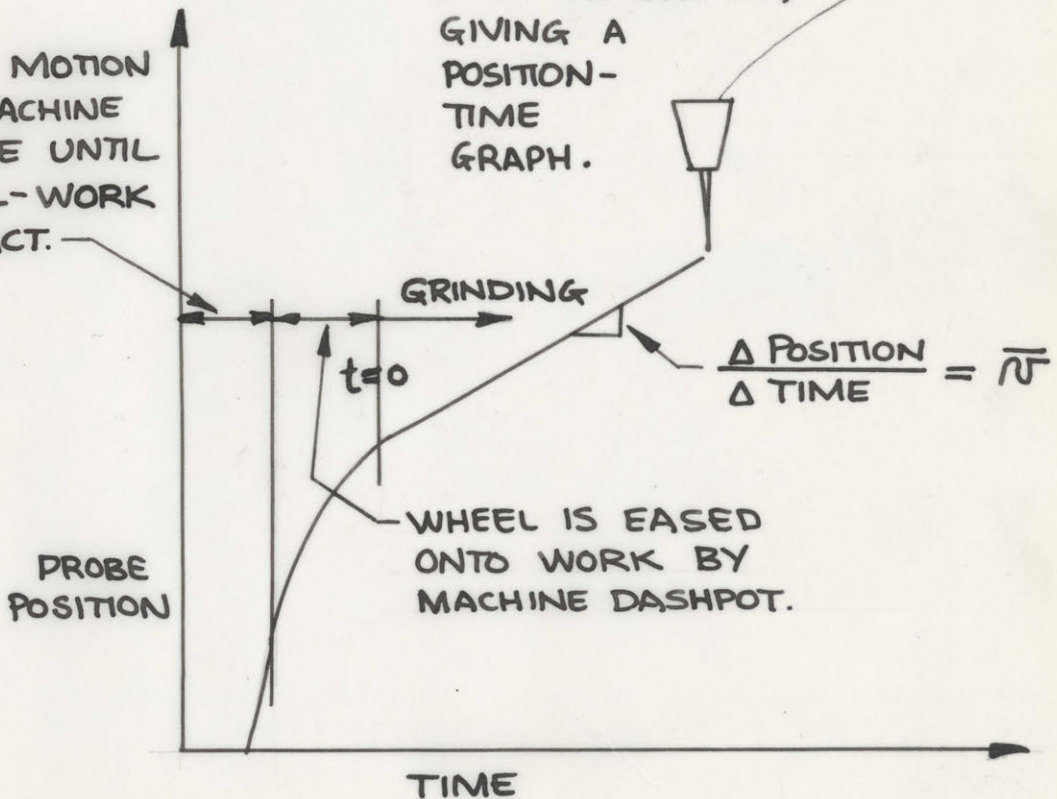


FIG. 11 MEASURING \bar{v}

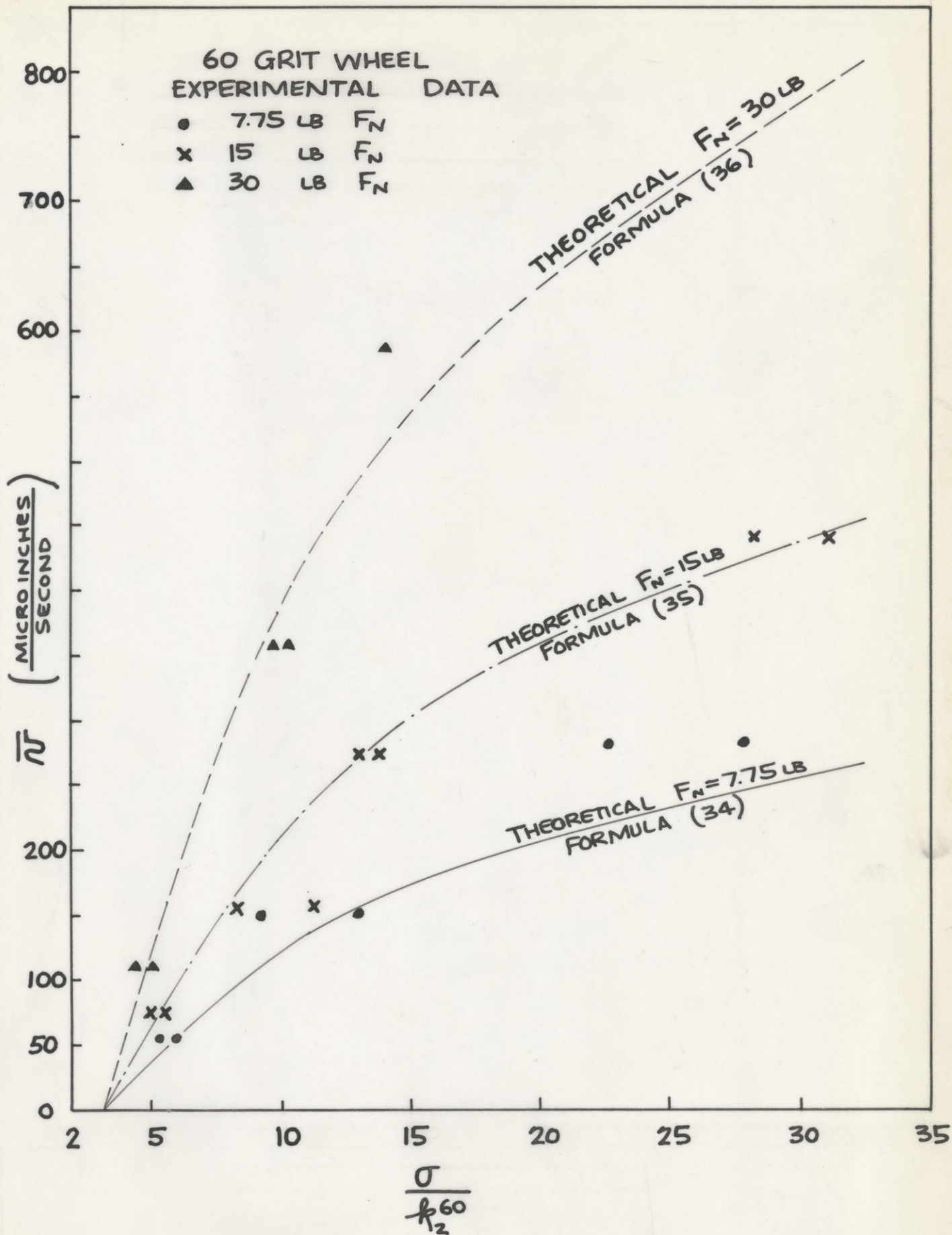


FIG. 12 EXP. AND THEOR. $\bar{\sigma}$ vs. $\frac{\sigma}{R_2^{60}}$

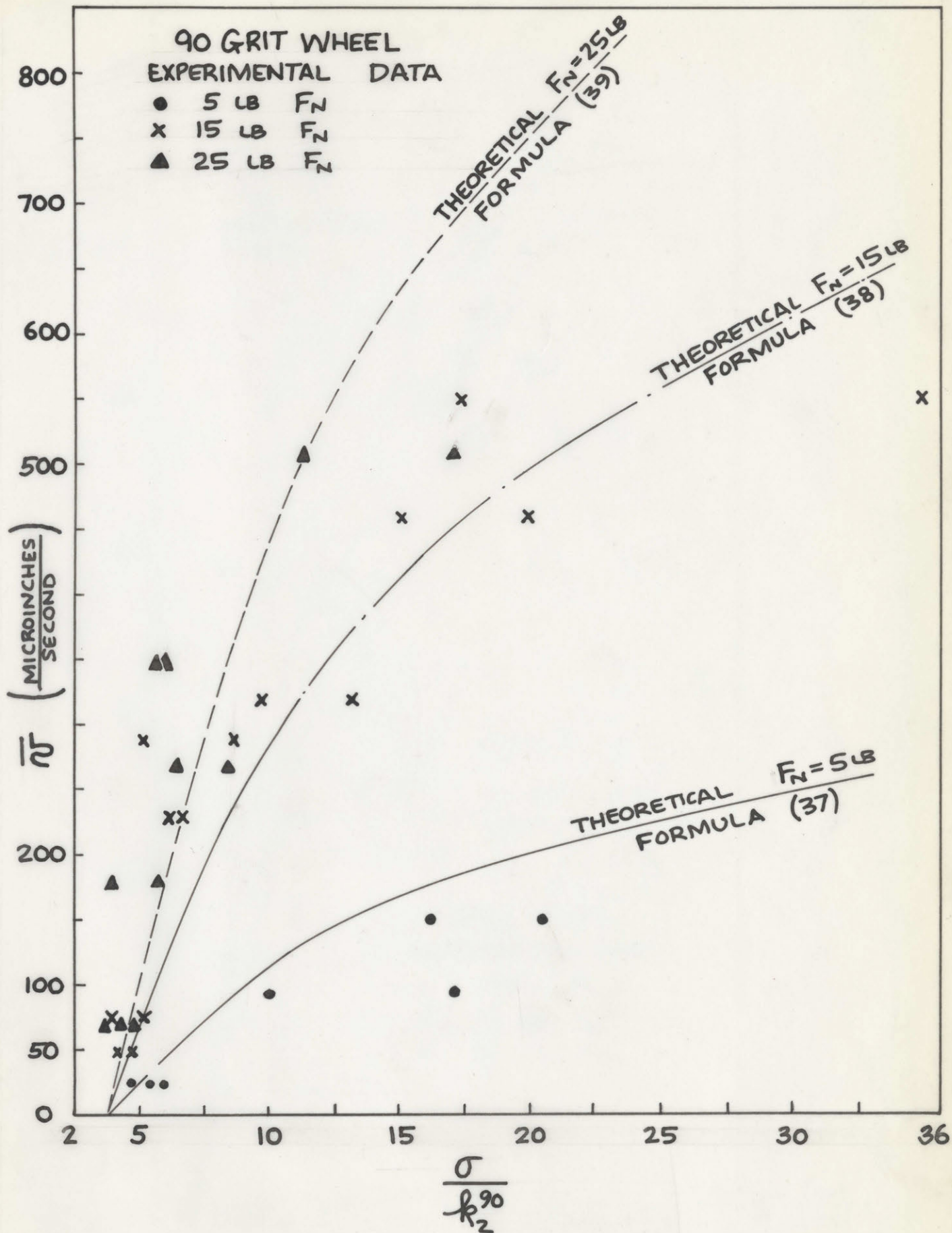


FIG. 13 EXP. AND THEOR. \bar{v} vs. $\frac{\sigma}{k_2^{90}}$

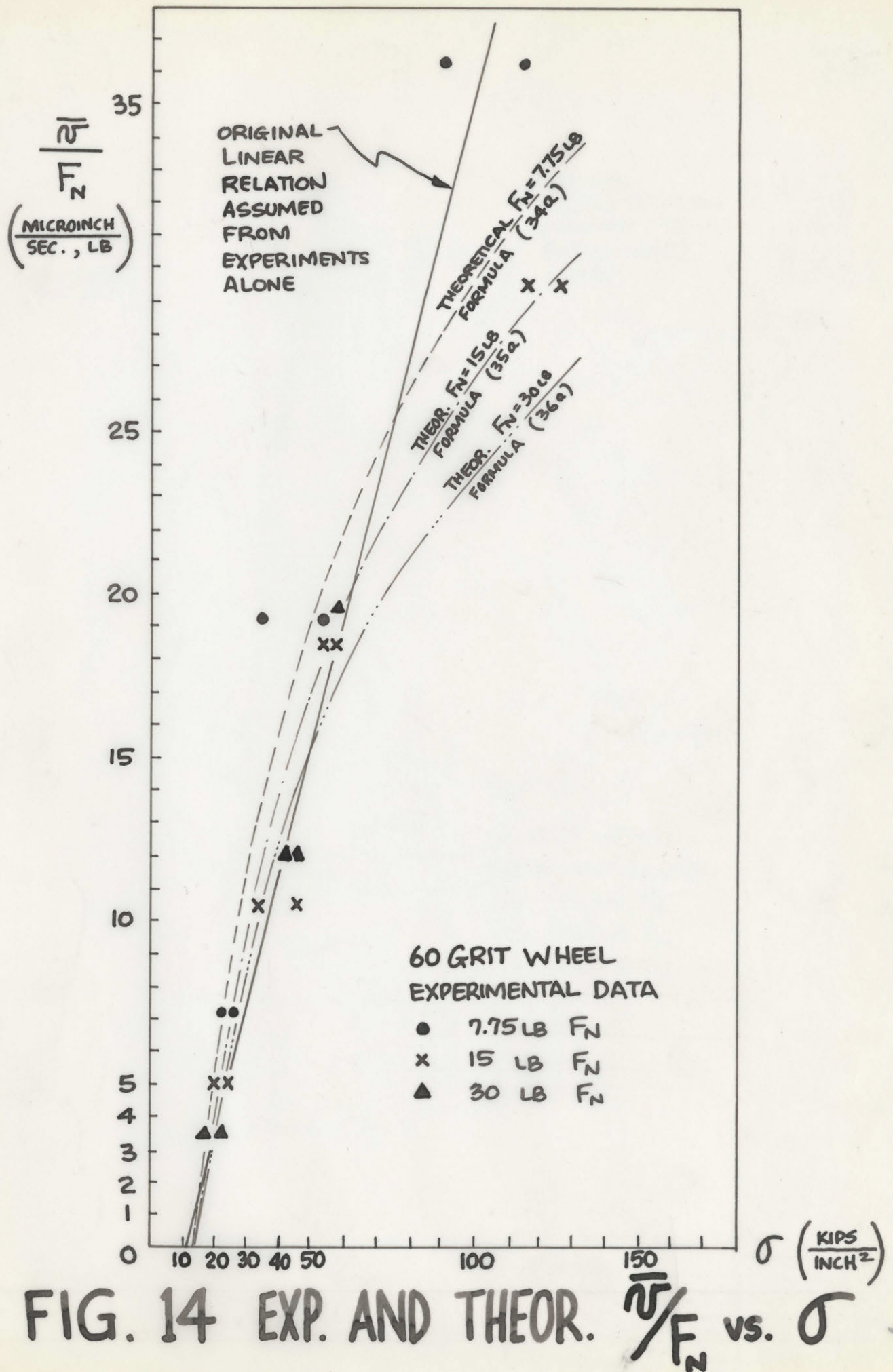


FIG. 14 EXP. AND THEOR. $\frac{\sqrt{F}}{F_N}$ vs. σ

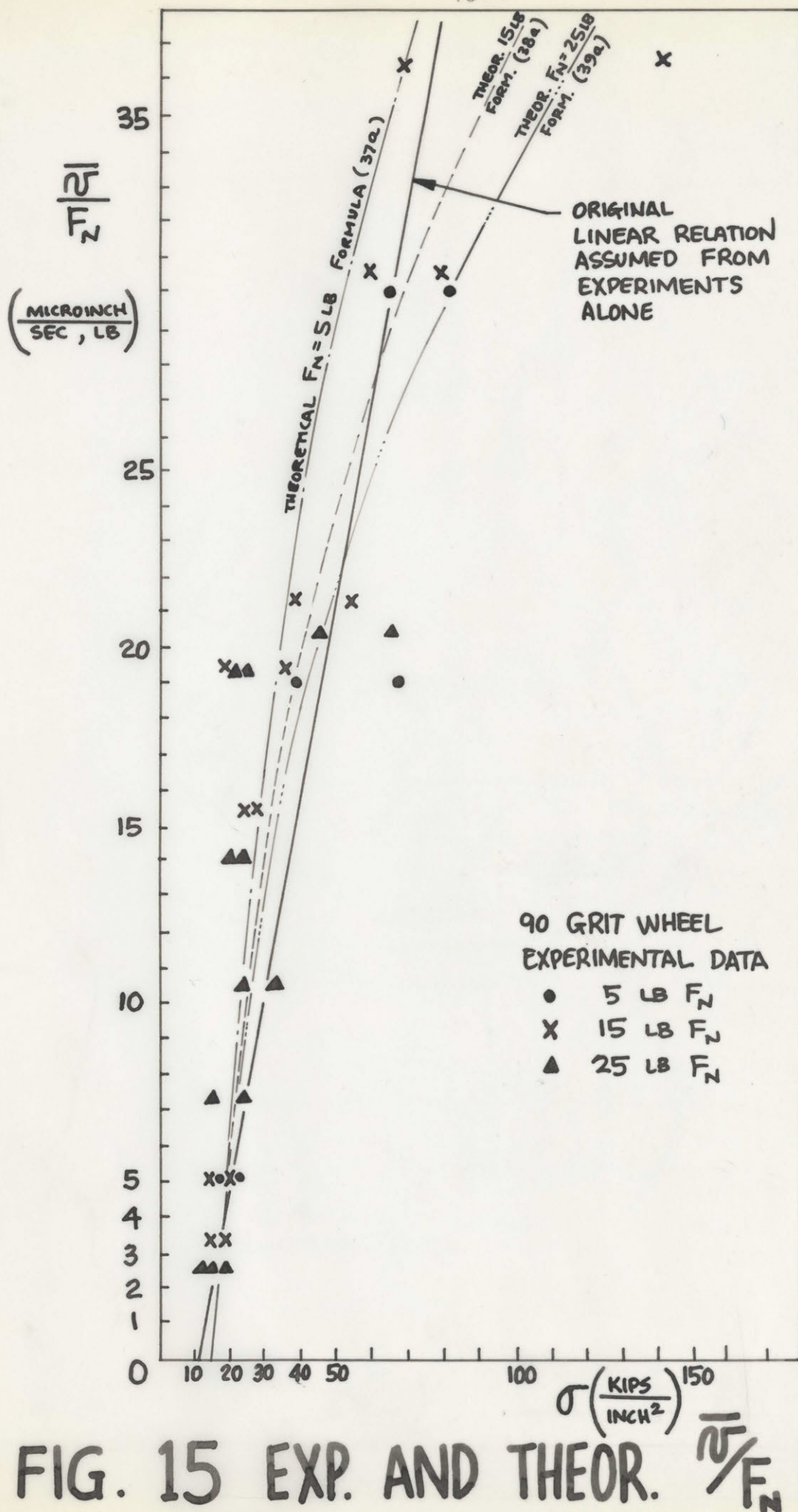


FIG. 15 EXP. AND THEOR. $\sqrt{R_a}/F_N$ vs. σ

FIG. 16 NSF LATHE ARRANGED FOR TESTS USING SINGLE GRAINS

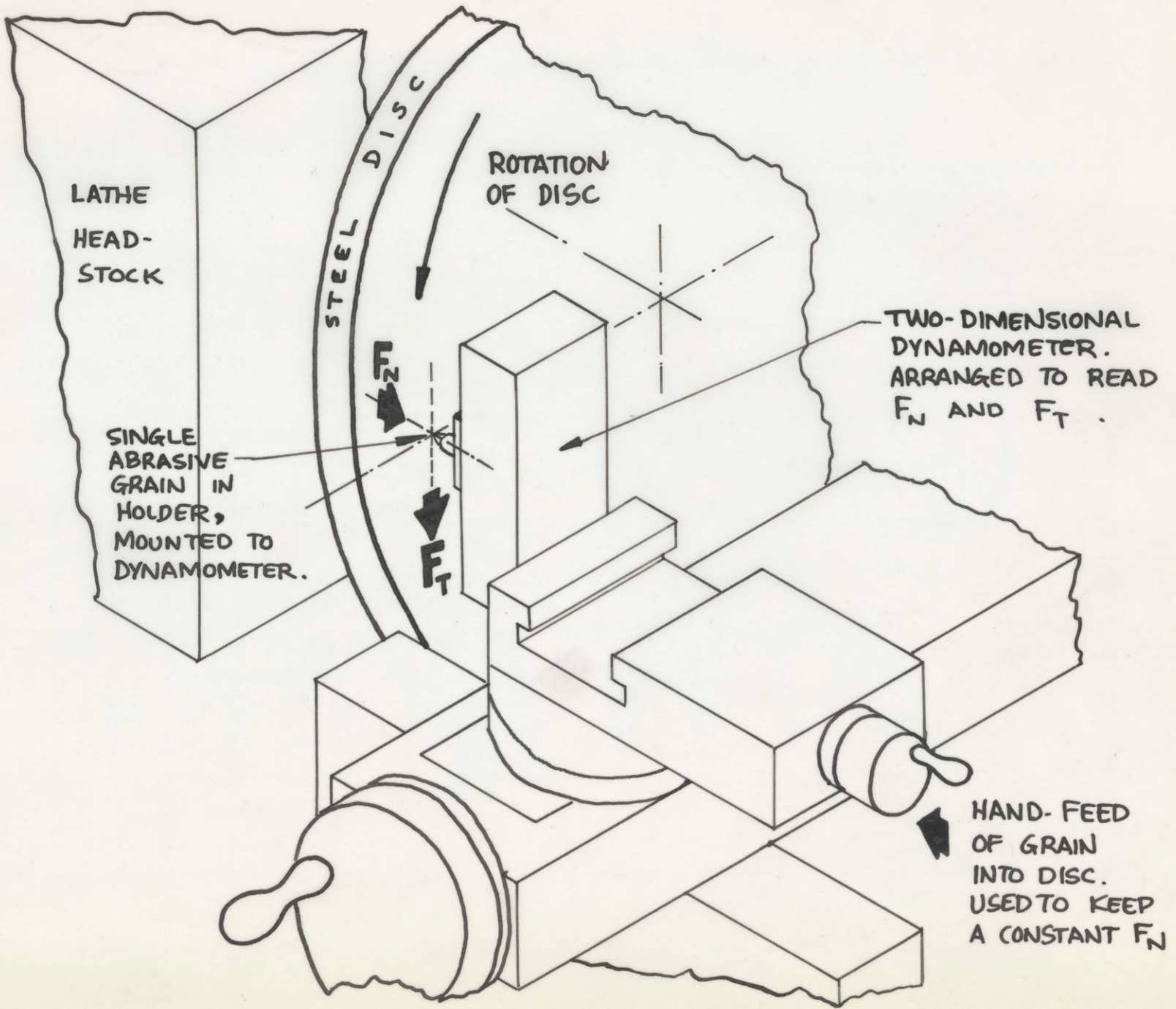
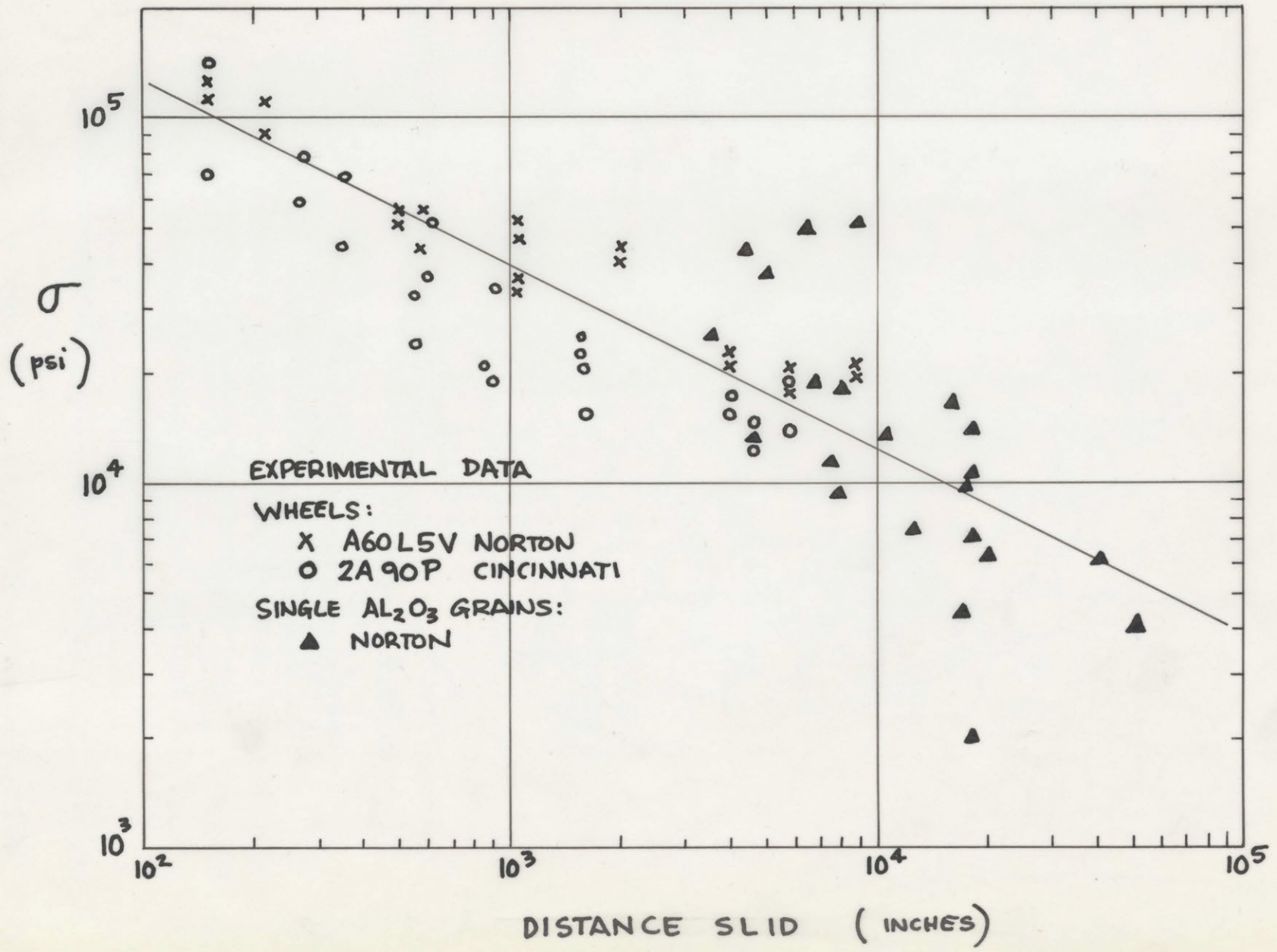
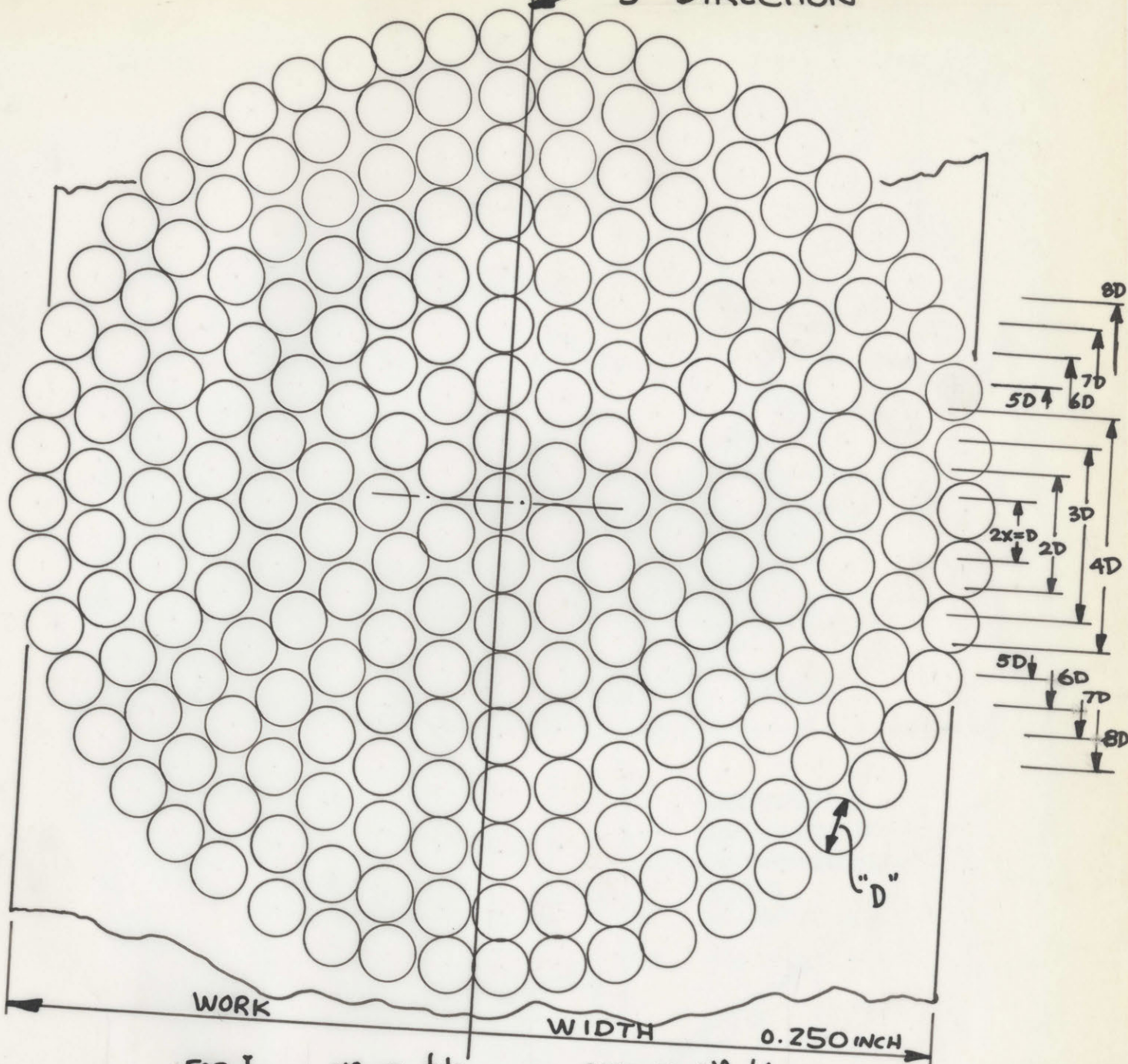


FIG. 17 VARIOUS TESTS σ vs. DISTANCE

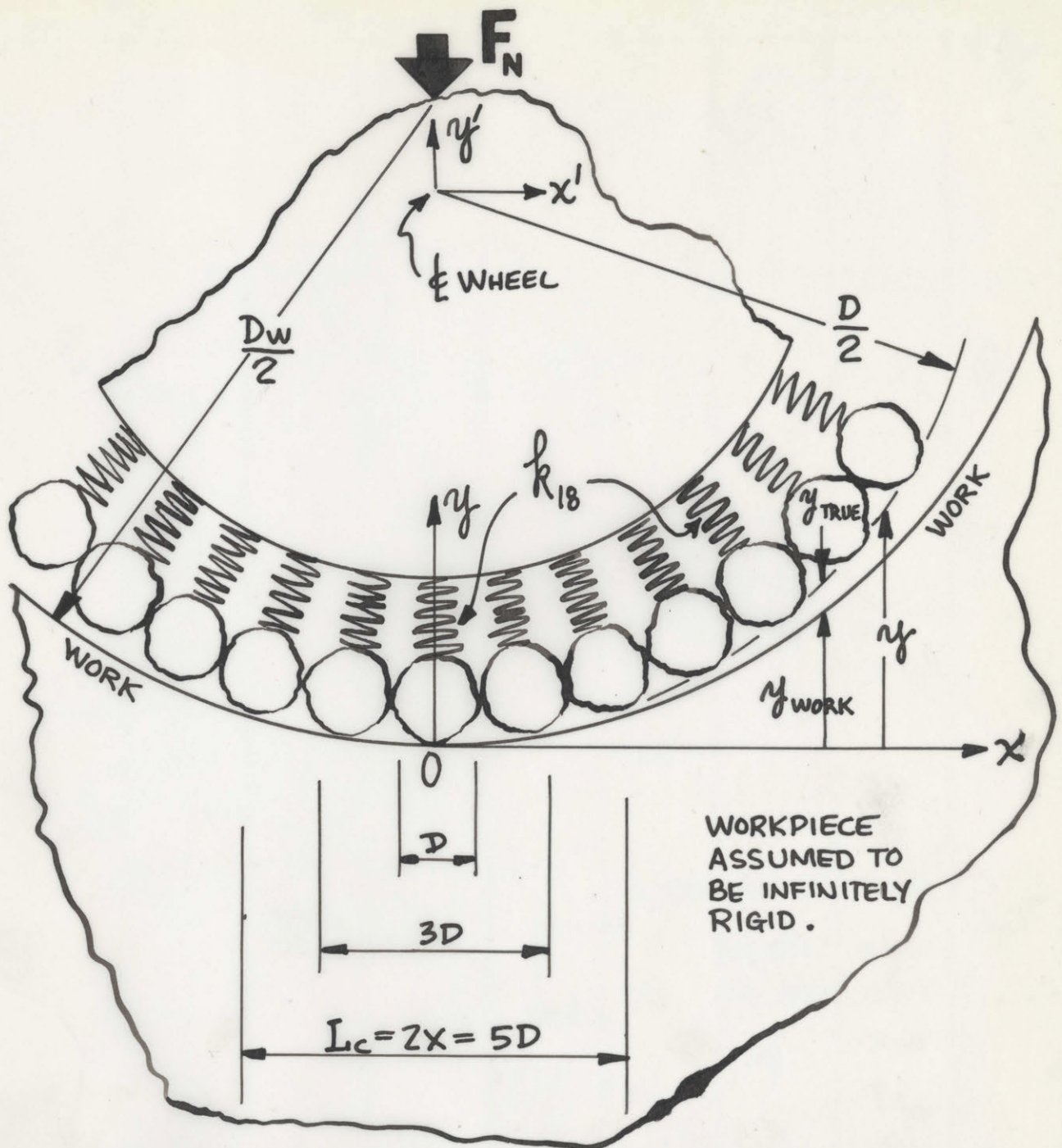




FOR L_c ($L_c = 2X$)	NO OF ϕ 's INTERCEPTED	RATIO OF NO ϕ 's INTERCEPTED (USING 18 AS 1)
D	18	1.00
2D	35	1.95
3D	50	2.78
4D	68	3.78
5D	83	4.60
6D	99	5.50
7D	114	6.35
8D	132	7.35

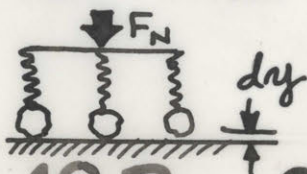
THE ABOVE FIGURE IS FOR 60 GRIT ($D = 0.016$ INCH). SHOWN 25X SIZE

FIG. 18A ARRAY OF GRAINS



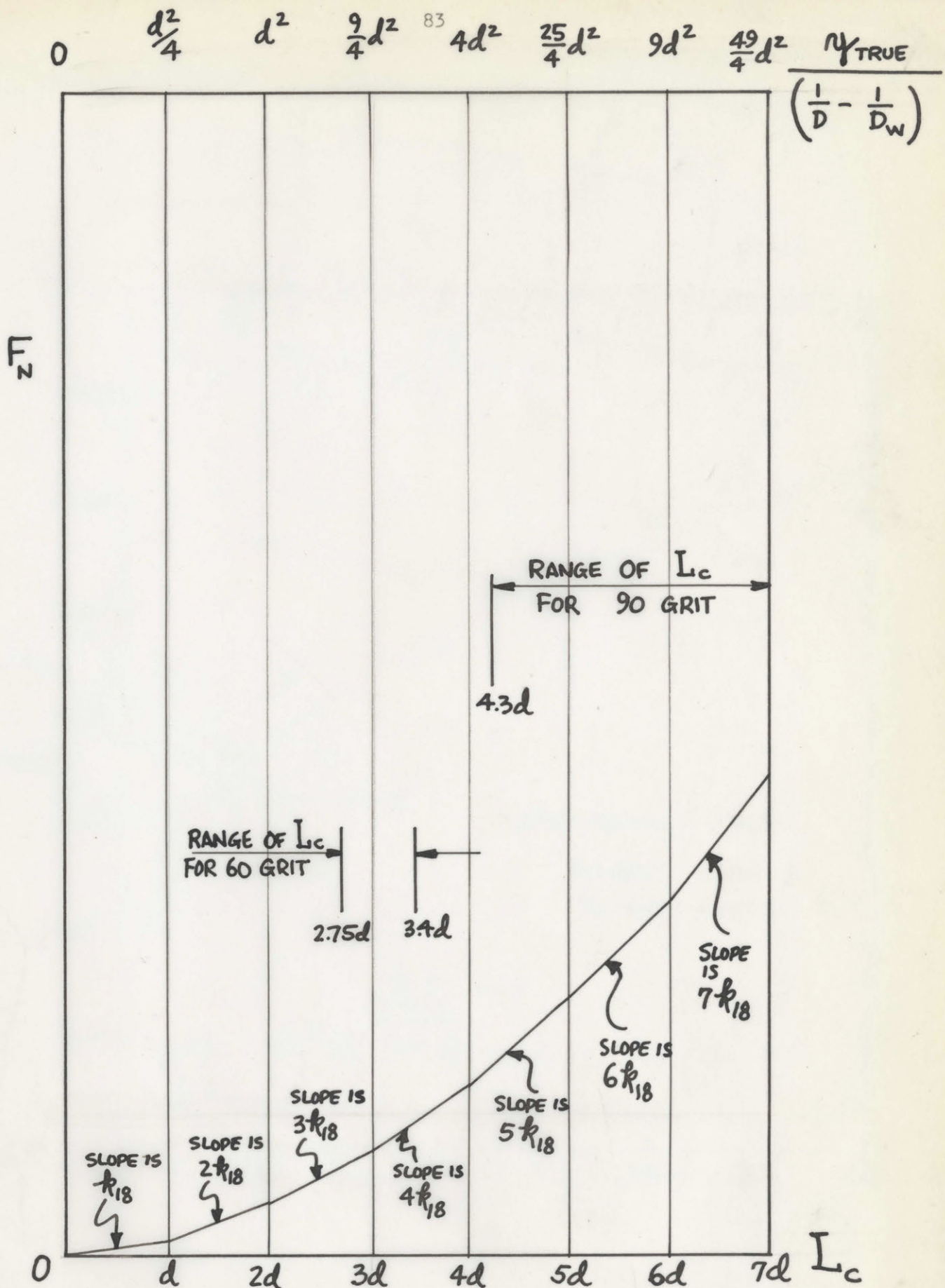
ABOVE PICTURE REPRESENTS A PLANE THRU THE WHEEL AND WORK. EACH GRAIN SHOWN REPRESENTS A ROW OF 18 GRAINS. THEN EACH ROW CAN BE CONSIDERED TO BE ONE GRAIN MOUNTED ON A SPRING OF STIFFNESS k_{18} .

THEN FOR THREE ROWS IN CONTACT ($L_c = 2x = 3D$):



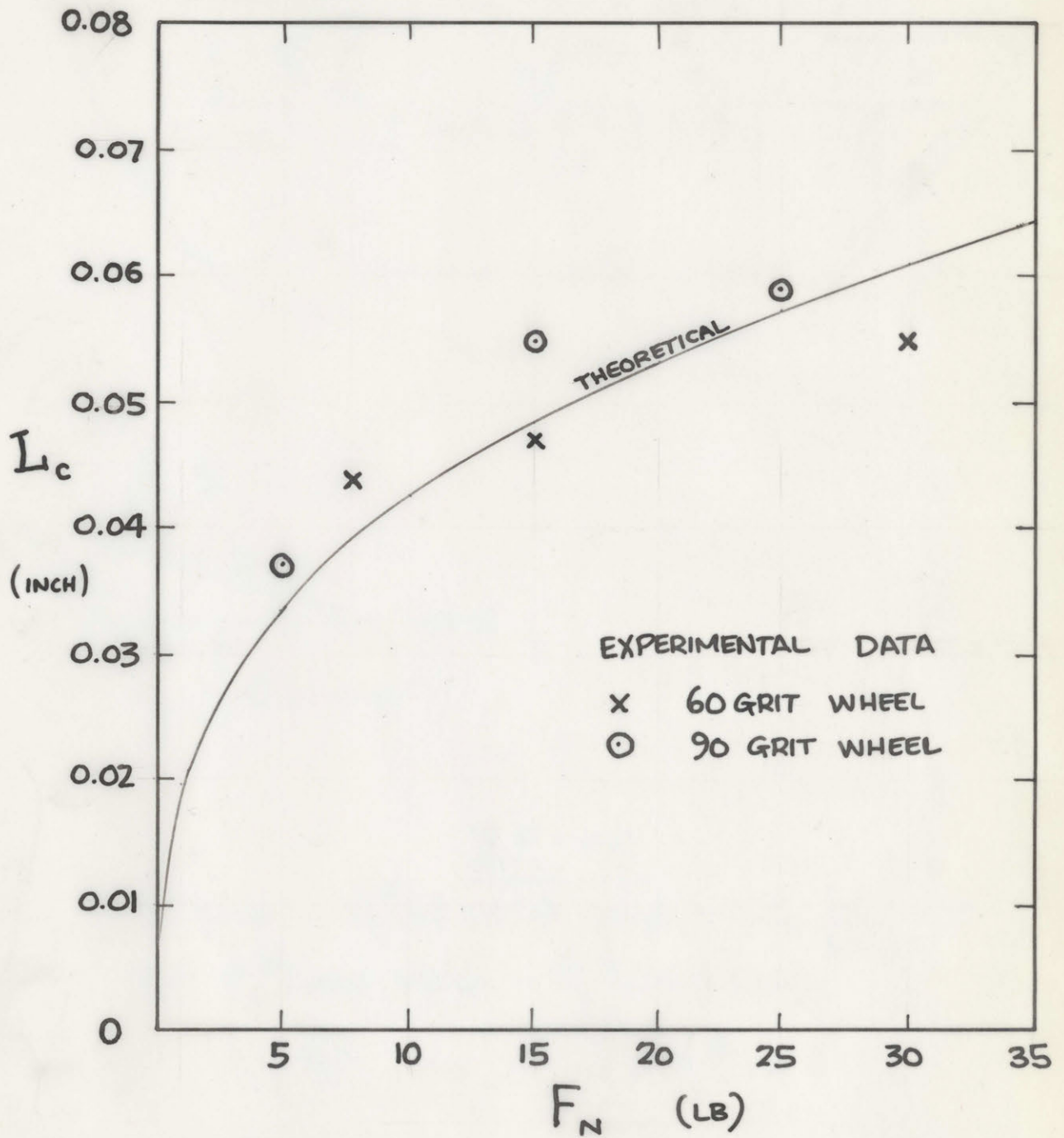
$$dF = 3k_{18} \text{ dry}$$

FIG. 18 B SPRING MODEL OF WHEEL

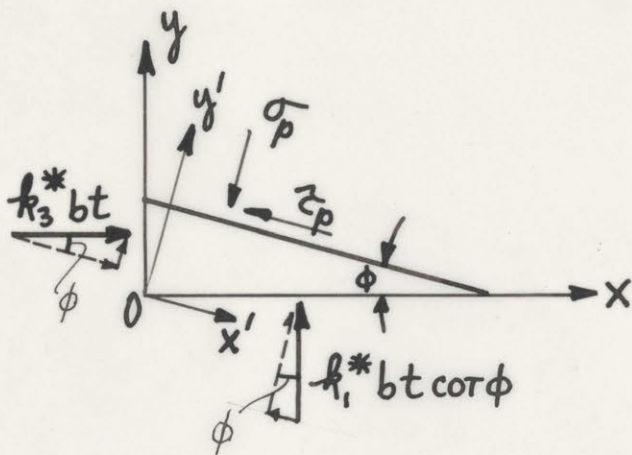
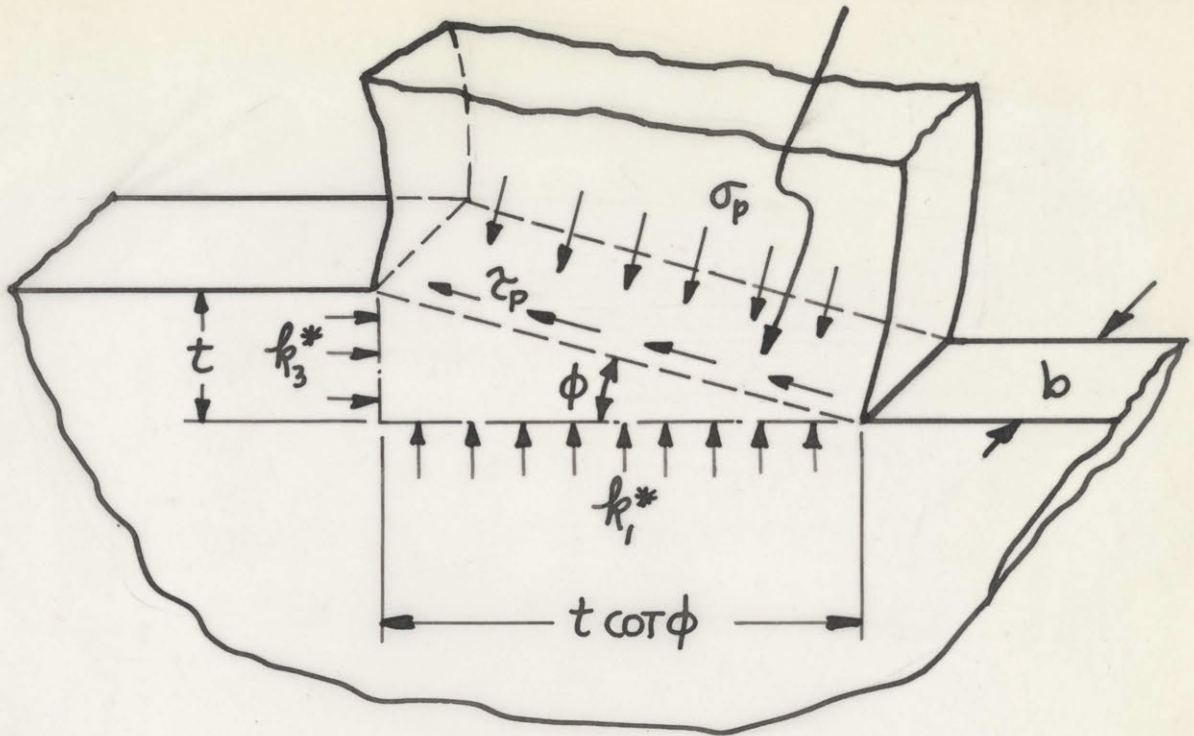


SINCE $y_T = \left[\frac{1}{D} - \frac{1}{D_w} \right] \left(\frac{L_c}{2} \right)^2$, CAN CALL ABCISSA L_c AS ABOVE

FIG. 18C F_N vs. y_{TRUE} OR F_N vs. L_c

FIG. 18 D EXP. AND THEOR. L_c vs. F_N

$$\text{AREA OF SHEAR PLANE} = \frac{bt}{\sin \phi}$$



$$\Sigma F'_x = 0$$

$$k_3^* bt \cos \phi - k_1^* bt \cot \phi \sin \phi - \tau_p \frac{bt}{\sin \phi} = 0$$

$$\tau_p = k_3^* \cos \phi \sin \phi - k_1^* \cos \phi \sin \phi$$

$$\text{BUT } k_3 = k_3^* \quad \text{AND} \quad k_1 = k_1^* \cot \phi$$

$$\therefore \tau_p = k_3 \cos \phi \sin \phi - k_1 \frac{\cos \phi \sin \phi}{\cot \phi}$$

$$\tau_p = k_3 \cos \phi \sin \phi - k_1 \sin^2 \phi$$

FIG. 19 SHEAR-PLANE RELATIONS